CANADIAN THESES ON MICROFICHE

I.S.B.N.

THESES CANADIENNES SUR MICROFICHE

National Library of Canada
Collections Development Branch

Canadian Theses on
Microfiche Service

Ottawa, Canada
K1A 0N4

Bibliothèque nationale du Canada
Direction du développement des collections

Service des thèses canadiennes
sur microfiche

## NOTICE

The quality of this microfiche is heavily dependent upon the quality of the original thesis submitted for microfilming. Every effort has been made to ensure the highest quality of reproduction possible.

If pages are missing, contact the university which granted the degree.

Some pages may have indistinct print especially if the original pages were typed with a poor typewriter ribbon or if the university sent us a poor photocopy.

Previously copyrighted materials (journal articles, published tests, etc.) are not filmed.

Reproduction in full or in part of this film is governed by the Canadian Copyright Act, R.S.C. 1970, c. C-30. Please read the authorization forms which accompany this thesis.

THIS DISSERTATION
HAS BEEN MICROFILMED
EXACTLY AS RECEIVED

## AVIS

La qualité de cette microfiche dépend grandement de la qualité de la thèse soumise au microfilmage. Nous avons tout fait pour assurer une qualité supérieure de reproduction.

S'il manque des pages, veuillez communiquer avec l'université qui a conféré le grade.

La qualité d'impression de certaines pages peut laisser à désirer, surtout si les pages originales ont été dactylographiées à l'aide d'un ruban usé ou si l'université nous a fait parvenir une photocopie de mauvaise qualité.

Les documents qui font déjà l'objet d'un droit d'auteur (articles de revue, examens publiés, etc.) ne sont pas microfilmés.

La reproduction, même partielle, de ce microfilm est soumise à la Loi canadienne sur le droit d'auteur, SRC 1970, c. C-30. Veuillez prendre connaissance des formules d'autorisation qui accompagnent cette thèse.

LA THÈSE A ÉTÉ
MICROFILMÉE TELLE QUE
NOUS L'AVONS REÇUE

NL-339 (r. 82/08)

Canada

53

0-315-15962-6

National Library of Canada | Bibliothèque nationale du Canada

Canadian Theses Division | Division des thèses canadiennes

Ottawa, Canada
K1A 0N4

63871

## PERMISSION TO MICROFILM — AUTORISATION DE MICROFILMER

• Please print or type — Écrire en lettres moulées ou dactylographier

Full Name of Author — Nom complet de l'auteur

BOHDAN KOCHTUBAJDA

| Date of Birth — Date de naissance | Country of Birth — Lieu de naissance |
|---|---|
| OCTOBER 1, 1954 | CANADA |

Permanent Address — Résidence fixe

69 PEACE RIVER DRIVE
C/O BOX 1131
DEVON, ALBERTA T0C1E0

Title of Thesis — Titre de la thèse

THEORY AND MEASUREMENT OF DRY ICE SUBLIMATION IN CLEAR AIR AND SIMULATED CLOUD.

University — Université

UNIVERSITY OF ALBERTA

Degree for which thesis was presented — Grade pour lequel cette thèse fut présentée

M SC

| Year this degree conferred — Année d'obtention de ce grade | Name of Supervisor — Nom du directeur de thèse |
|---|---|
| 1983 | DR. G. P. LOZOWSKI |

Permission is hereby granted to the NATIONAL LIBRARY OF CANADA to microfilm this thesis and to lend or sell copies of the film.

The author reserves other publication rights, and neither the thesis nor extensive extracts from it may be printed or otherwise reproduced without the author's written permission.

L'autorisation est, par la présente, accordée à la BIBLIOTHÈQUE NATIONALE DU CANADA de microfilmer cette thèse et de prêter ou de vendre des exemplaires du film.

L'auteur se réserve les autres droits de publication; ni la thèse ni de longs extraits de celle-ci ne doivent être imprimés ou autrement reproduits sans l'autorisation écrite de l'auteur.

| Date | Signature |
|---|---|
| March 25, 1983 | B. Kochtubajda |

NL-91 (4/77)

THE UNIVERSITY OF ALBERTA

# THEORY AND MEASUREMENT OF DRY ICE SUBLIMATION IN CLEAR AIR AND SIMULATED CLOUD

by

BOHDAN KOCHTUBAJDA

(C)

A THESIS

SUBMITTED TO THE FACULTY OF GRADUATE STUDIES AND RESEARCH

IN PARTIAL FULFILMENT OF THE REQUIREMENTS FOR THE DEGREE

OF MASTER OF SCIENCE

IN

METEOROLOGY

DEPARTMENT OF GEOGRAPHY

EDMONTON, ALBERTA

SPRING, 1983

THE UNIVERSITY OF ALBERTA

RELEASE FORM

NAME OF AUTHOR Bohdan Kochtubajda

TITLE OF THESIS Theory and Measurement of Dry Ice Sublimation In Clear Air and Simulated Cloud

DEGREE FOR WHICH THESIS WAS PRESENTED Master of Science

YEAR THIS DEGREE GRANTED 1983

Permission is hereby granted to THE UNIVERSITY OF ALBERTA LIBRARY to reproduce single copies of this thesis and to lend or sell such copies for private, scholarly or scientific research purposes only.

The author reserves other publication rights, and neither the thesis nor extensive extracts from it may be printed or otherwise reproduced without the author's written permission.

(Signed) B. Kochtubajda

PERMANENT ADDRESS:

69 Peace River Drive
c/o Box 1131
Devon, Alberta
T0C 1E0

DATED March 25 1983

THE UNIVERSITY OF ALBERTA

FACULTY OF GRADUATE STUDIES AND RESEARCH

The undersigned certify that they have read, and recommend to the Faculty of Graduate Studies and Research, for acceptance, a thesis entitled "Theory and Measurement of Dry Ice Sublimation in Clear Air and Simulated Cloud" submitted by Bohdan Kochtubajda in partial fulfilment of the requirements for the degree of Master of Science in Meteorology.

Edward J. Stadnyk
.....
Supervisor

E.M. Yates.....

Robert T. Clarkson.....

Date ..Mar. 15/83....

## DEDICATION

To my wife, Lillian, and sons, Matthew and Andrew.

For their love and understanding.

To my parents.

For their love and encouragement over these years.

## ABSTRACT

A numerical model incorporating heat transfer theory with cylindrical geometry has been developed to investigate the sublimation rate of dry ice pellets in clear air and simulated cloud. A series of thirty two experiments were conducted in the University of Alberta FROST icing-wind tunnel, and nine aircraft drop experiments were performed to verify model predictions of the sublimation rate.

The principal conclusions drawn from this study are: (a) The FROST icing wind tunnel is an appropriate facility for conducting sublimation rate experiments, and may also be useful for investigations into ice crystal production rates. (b) In spite of the use of several simplifying assumptions, the cylindrical model predicts the sublimation rates of dry ice pellets to within 10%, when compared with wind tunnel observations. (c) The model predicts the fall times of cylindrical pellets to within 10%-15%, when compared with the free-fall experiments. (d) Cloudy and saturated conditions, with high temperatures, enhance the sublimation rate of dry ice but, cloudy and saturated conditions, with cold temperatures do not make an appreciable effect on the sublimation rate of dry ice. (e) Numerical simulations of freely-falling pellets suggest pellets with diameters of between 0.5 and 0.6 cm for efficient use of dry ice when dropped from the -10 °C level.

## ACKNOWLEDGEMENTS

I am grateful to various people and organizations whose cooperation and support have enabled me to complete this thesis.

I am indebted to my departmental supervisor, Dr. E. P. Lozowski, for his guidance, his many helpful suggestions, his assistance with the experiments, and for his thorough review of this manuscript.

I am grateful to Dr. T. E. Gates of the Department of Mechanical Engineering for his kindness in making the FROST tunnel facility available, for assisting me in its use, and for serving on my examining committee.

I wish to thank Dr. R. B. Charlton who, with Dr. Lozowski and Dr. Gates, served on my examining committee.

I am grateful to the staff of the Atmospheric Sciences Department of the Alberta Research Council for their cooperation. In particular, I would like to thank Dr. M. English for giving me the opportunity to conduct this work. I am grateful to Dr. L. Cheng who assisted in the free-fall experiments. I would also like to thank Dr. B. L. Barge for allowing me to use the departmental computer to generate this report.

I am also grateful to Intera Environmental Consultants Ltd. for providing an aircraft and pilots during their busy seeding operations. In particular, I would like to acknowledge Mr. Ken Grandia, Mr. Ian Macgregor and Ms. Sandi Holliday.

Finally, I wish to thank Ms. Barb Henderson who prepared the diagrams, Ms. Maria Tatchyn who typed the equations, and Mr. John Gertz who prepared the photograph.

The financial support from Alberta Agriculture and the Alberta Research Council for the computing resources is gratefully acknowledged.

TABLE OF CONTENTS


| | PAGE |
|---|---|
| DEDICATION | iv |
| ABSTRACT | v |
| ACKNOWLEDGEMENTS | vi |
| TABLE OF CONTENTS | viii |
| LIST OF TABLES | x |
| LIST OF FIGURES | xi |
| LIST OF SYMBOLS | xiv |

| CHAPTER | PAGE |
|---|---|
| 1. INTRODUCTION | 1 |
| 2. THE THEORETICAL MODEL | 5 |
| 2.1 Theoretical Model Description | 5 |
| 2.2 Sensitivity Tests | 10 |
| 3. THE WIND TUNNEL EXPERIMENTS | 12 |
| 3.1 FROST Tunnel Capabilities | 12 |
| 3.2 Experimental Procedure | 14 |
| 3.3 Experimental Observations at High Temperatures | 20 |
| 3.4 Experimental Observations at Low Temperatures | 32 |

CHAPTER PAGE

4. THE FREE-FALL EXPERIMENTS..... 44

4.1 Free-Fall Model Description..... 44

4.2 The Free-Fall Experiments..... 45

4.3 A Free-Fall Simulation..... 47

5. SUMMARY CONCLUSIONS AND RECOMMENDATIONS..... 51

BIBLIOGRAPHY..... 53

APPENDICES

A Determination of the Nusselt Number from Experimental Observations..... 56

B Derivation of the $Q_{es}$ term..... 59

C An Order of Magnitude Analysis of the Heat Balance Equation.... 63

D Analytic Solution to Sublimation Rate Expression..... 66

E Derivation of the Terminal Velocity for a Cylindrical Object... 68

F Computer Program Listings..... 71

## LIST OF TABLES


| TABLE | | PAGE |
|---|---|---|
| 1 | Sensitivity test results..... | 11 |
| 2 | Summary of Experimental Conditions..... | 19 |
| 3 | The Drag Coefficient of Truncated Circular Cylinders..... | 45 |

## LIST OF FIGURES


| FIGURE | | PAGE |
|---|---|---|
| 1 | A plan view of the FROST icing wind tunnel..... | 13 |
| 2 | The analyzed cross-sections of a dry ice pellet..... | 15 |
| 3 | A dry ice pellet suspended in cloudy air, in the FROST tunnel. The wake is clearly visible..... | 18 |
| 4 | A comparison of theory and experiment at warm temperature with the sprays off. The heavy lines are the theoretical prediction, and the jagged lines are the experimental observations. The conditions for experiment 3 were: 28 $ms^{-1}$ ,26.5 °C. The conditions for experiments 4 and 5 were: 14 $ms^{-1}$ ; 18.5 °C..... | 23 |
| 5 | Same as Figure 4. Conditions for experiment 19 were; 14 $ms^{-1}$ , 24.0 °C..... | 24 |
| 6 | Same as Figure 4. Conditions for experiments 20 and 21 were; 14 $ms^{-1}$ , 32.5 °C..... | 24 |
| 7 | Same as Figure 4. Conditions for experiment 26 were; 14 $ms^{-1}$ , 28.5 °C..... | 25 |
| 8 | Same as Figure 4. Conditions for experiment 27 were; 16 $ms^{-1}$ , 31.0 °C..... | 26 |
| 9 | Same as Figure 4. Conditions for experiment 28 were; 16 $ms^{-1}$ , 33.0 °C..... | 27 |
| 10 | Same as Figure 4. Conditions for experiment 29 were; 16 $ms^{-1}$ , 34.6 °C..... | 27 |
| 11 | Same as Figure 4. Conditions for experiment 30 were; 16 $ms^{-1}$ , 35.5 °C..... | 28 |
| 12 | Same as Figure 4. Conditions for experiments 31 and 32 were; 31 $ms^{-1}$ , 37.5 °C..... | 29 |

FIGURE PAGE

13 A comparison of theory and experiment at warm temperatures with the sprays on. The heavy lines are the theoretical prediction, and the jagged lines are the experimental results. The conditions for experiments 6 and 7 were: 14 $ms^{-1}$, 19.5 °C. LWC was not available..... 29

14 Same as Figure 13. Conditions for experiments 22 and 23 were; 14 $ms^{-1}$, 32.5 °C, 3.08 $gm^{-3}$..... 30

15 Same as Figure 13. Conditions for experiments 24 and 25 were; 14$ms^{-1}$, 34.0 °C, 0.46 $gm^{-3}$..... 31

16 A comparison of theory and experiment at cold temperatures with the sprays off. The heavy lines are the theoretical prediction, and the jagged lines are the experimental observations. The conditions for experiments 8, 9, and 14 were: 13 $ms^{-1}$, -10 °C..... 35

17 Same as Figure 16. Conditions for experiments 15 and 16 were: 13 $ms^{-1}$, -11 °C..... 36

18 A comparison of theory and experiment at cold temperatures with the sprays on. The heavy lines are the theoretical prediction, and the jagged lines are the experimental observations. The conditions for experiments 10, 11, 12, and 13 were: 13 $ms^{-1}$, -10 °C, 0.45 $gm^{-3}$, 0.38 $gm^{-3}$, 1.40 $gm^{-3}$, and 1.72 $gm^{-3}$, respectively..... 37

19 Same as Figure 18. Conditions for experiments 17 and 18 were: 13 $ms^{-1}$, -11 °C, 0.42 $gm^{-3}$, and 0.65 $gm^{-3}$, respectively..... 38

20 Summary of Theoretical model. The solid line represents a dry environment. The dashed line represents a cloudy environment. All cases were run using a velocity of 14 $ms^{-1}$..... 39

FIGURE PAGE


21 Same as Figure 11. Theoretical prediction determined using a dry ice surface temperature of -78 °C..... 40

22 Same as Figure 15. Theoretical prediction determined using a dry ice surface temperature of -78 °C..... 41

23 Same as Figure 16. Theoretical prediction determined using a dry ice surface temperature of -78 °C..... 42

24 Same as Figure 18. Theoretical prediction determined using a dry ice surface temperature of -78 °C..... 43

25 Model predictions for the free-fall experiments. The solid lines are the pellet diameter as a function of height for three release heights. The dashed lines are the isochrones in seconds..... 49

26 A simulation of dry ice seeding. The solid lines are the pellet diameter as a function of height or temperature. The dashed lines are isochrones in seconds..... 50

27 Scatter Diagram of Nusselt Calculations..... 58

## LIST OF SYMBOLS


| SYMBOL | | PAGE |
|---|---|---|
| $C_D$ | Drag coefficient | 44 |
| $c_i$ | Specific heat capacity of ice ($Jkg^{-1}K^{-1}$) | 8 |
| $c_p$ | Specific heat capacity of dry air at constant pressure ($Jkg^{-1}K^{-1}$) | 7 |
| $c_w$ | Specific heat capacity of water ($Jkg^{-1}K^{-1}$) | 8 |
| D | Cylinder diameter (m) | 6 |
| e | Partial pressure of water vapor (mb) | 59 |
| $e_a(t_a)$ | Saturation vapor pressure of water at the ambient air temperature (mb) | 7 |
| $e_s(t_s)$ | Saturation vapor pressure of water at the surface temperature (mb) | 7 |
| E | Collection efficiency | 64 |
| $F_D$ | Drag force (J) | 68 |
| g | Acceleration due to gravity ($ms^{-2}$) | 44 |
| h | Heat transfer coefficient ($Wm^{-2}{}^{o}C^{-1}$) | 6 |
| $k_a$ | Thermal conductivity of air ($Wm^{-2}{}^{o}C^{-1}$) | 6 |
| $l_s$ | Specific latent heat of sublimation of water vapor ($Jkg^{-1}$) | 7 |
| L | Cylinder length (m) | 6 |
| $L_f$ | Specific latent heat of freezing of water ($Jkg^{-1}$) | 8 |
| $L_\delta$ | Specific latent heat of sublimation of dry ice ($Jkg^{-1}$) | 7 |
| m | Total mass of dry ice pellet (kg) | 7 |
| Nu | Nusselt number | 6 |
| p | Partial pressure of dry air (mb) | 59 |
| P | Static pressure in the free stream (mb) | 7 |
| Pr | Prandtl number for air | 7 |

| SYMBOL | | PAGE |
|---|---|---|
| $Q_c$ | Total sensible heat transfer by conduction and convection (W) | 5 |
| $Q_d$ | Total sensible and latent heat transfer due to the cooling and freezing of impacting water droplets (W) | 5 |
| $Q_{es}$ | Total latent heat transfer due to sublimation of water vapor (W) | 5 |
| $Q_r$ | Total heat transfer due to radiation (W) | 5 |
| $Q_s$ | Total latent heat transfer due to sublimation of dry ice (W) | 5 |
| $R'$ | Specific gas constant for dry air ($Jkg^{-1}K^{-1}$) | 59 |
| $R_v$ | Specific gas constant for water vapor ($Jkg^{-1}K^{-1}$) | 59 |
| $R_w$ | Mass flux of droplets collected per unit time ($kgs^{-1}$) | 8 |
| Re | Reynolds number | 6 |
| Sc | Schmidt number for air | 7 |
| Sh | Sherwood number | 60 |
| $t_a$ | Ambient air temperature (°C) | 6 |
| $t_s$ | Surface temperature of dry ice pellet (°C) | 6 |
| $T_a$ | Ambient air temperature ( K) | 8 |
| $T_s$ | Surface temperature of dry ice pellet ( K) | 8 |
| V | Airspeed or fallspeed of the pellet ($ms^{-1}$) | 16 |
| w | Liquid water content ($kgm^{-3}$) | 64 |

| SYMBOL | | PAGE |
|---|---|---|
| $\Delta p$ | Dynamic pressure (in. of water) | 16 |
| $\Delta t$ | Time step (sec) | 11 |
| $\mathcal{D}_{wa}$ | Diffusivity of water vapor in air ($m^2 s^{-1}$) | 60 |
| $\varepsilon$ | Ratio of molecular weights of water vapor and dry air | 7 |
| $\varepsilon_a$ | Emissivity of air | 8 |
| $\varepsilon_s$ | Emissivity of dry ice | 8 |
| $\kappa$ | Thermal diffusivity of air ($m^2 s^{-1}$) | 61 |
| $\mu_a$ | Dynamic viscosity of air ($kgm^{-1} s^{-1}$) | 63 |
| $\nu$ | Kinematic viscosity of air ($m^2 s^{-1}$) | 61 |
| $\rho_a$ | Density of air ($kgm^{-3}$) | 16 |
| $\rho_c$ | Density of dry ice ($kgm^{-3}$) | 9 |
| $\sigma$ | Stefan-Boltzmann constant ($Wm^{-2}K^{-4}$) | 8 |

# CHAPTER 1

## INTRODUCTION

The manipulation of weather to his advantage has been a dream of man for many centuries. In its infancy, this ambition was limited to local need (rain for a patch of corn), and the methods were primitive (rain dances and lighting fires, Hess,1974). As knowledge of atmospheric processes increased, man's approach to this dream was directed toward scientific consideration of the possibilities of altering these processes.

The modern era of weather modification was initiated by Schaefer (1946), when dry ice (solid carbon dioxide), was serendipitously used in his efforts to discover a material to nucleate freezing in supercooled clouds. This event led to his discovery that dry ice can produce a host of ice embryos when inserted into a cloud. He observed that the concentrations produced by a tiny bit of dry ice were high and the ice crystals were very small. The mechanism by which dry ice produces large amounts of ice crystals in its wake while falling through a supercooled cloud was found to be homogeneous nucleation from the vapor phase.

The recent revival of the use of dry ice as an alternative cloud seeding agent, (Schaefer,1976; Holroyd et al.,1978; Silverman,1979; English and Marwitz,1981), has renewed interest in the sublimation rate of dry ice pellets. Knowledge of the sublimation rate, to accurately

predict the distance that dry ice pellets will fall, is essential if the dry ice is to be used efficiently in cloud seeding operations. With such information, an optimum pellet size may be selected for a given mission,( provided that the pellets can be produced to whatever specified size ). The sublimation rate is also an important parameter for numerical modellers to use in their studies simulating the effects of dry ice seeding on cumulus clouds (Kopp et al.,1979).

Some previous studies have been conducted to determine the sublimation rate of dry ice pellets. An investigation, (Mee and Eadie, 1963), was undertaken to find a means of increasing the efficiency of the dry ice cloud seeding process, and to develop field techniques and equipment for U.S Army personnel to dissipate whiteouts. Several experiments were conducted in a vertical wind-tunnel, to establish the time required for the complete sublimation of dry ice pellets of a given initial mass falling at their terminal velocities. From these measurements an empirical expression for the total sublimation of dry ice as a function of initial mass has been proposed.

Another study, (Fukuta, et al., 1971) was conducted to investigate the effectiveness (the number of ice crystals generated per gram of dry ice sublimed) of dry ice. Empirical equations for the sublimation rate of dry ice, terminal velocity and pellet surface temperature were obtained. Both of these studies have assumed the pellet geometry to be spherical, and they were limited to sublimation in clear air.

Summer cumulus cloud seeding experiments (English and Marwitz, 1981) have been conducted as part of the Alberta Hail Project since 1978. Three seeding treatments: dry ice pellets, silver iodide flares,

and placebos are applied to these clouds. The dry ice pellets used in these experiments have been obtained commercially in cylindrical form.

A few questions that needed to be resolved were: a) Wouldn't a sublimation rate expression based on cylindrical geometry be more appropriate to use for these experiments? b) Does a cloudy environment affect the sublimation rate of the dry ice? A study attempting to answer these questions was initiated, and the results are presented in this thesis.

The approach taken in this thesis is one which incorporates both theory and experiment in an attempt to examine the sublimation rate of cylindrical dry ice pellets both in clear air and simulated cloud. A description of the theory and the model will be presented in Chapter 2.

Laboratory experiments carried out in the University of Alberta's FROST icing-wind tunnel are discussed in Chapter 3. Their purpose was to test the the theoretical model. Descriptions of the FROST tunnel capabilities, the experimental procedures followed, and the data analysis techniques used are presented. The experimental results and comparisons with the theoretical model predictions of changes in diameter are also presented and discussed.

Several field experiments were conducted in which cylindrical dry ice pellets were dropped from an aircraft flying at a known altitude. These experiments are discussed in Chapter 4. The numerical model developed in Chapter 2 was modified slightly to investigate the sublimation of cylindrical dry ice pellets falling at terminal velocity through the atmosphere. The purpose of these experiments was to provide a check on the free-fall model predictions of the time taken to reach

the surface, and the final diameters the pellets achieve. A description of the free-fall model, and discussion of the results from these experiments are presented.

Conclusions and recommendations for future work are presented in Chapter 5.

# CHAPTER 2

# THE THEORETICAL MODEL

## 2.1 Theoretical Model Description

A theory is presented for the sublimation of fixed, cylindrical dry ice pellets in a moving, saturated (with respect to water) cloudy airstream. A heat flux balance (Lozowski et al. (1979)), at the surface of the cylindrical dry ice pellet is assumed. The heat balance equation can be expressed as:

$$Q_c + Q_{es} + Q_s + Q_r + Q_d = 0 \qquad (1)$$

where $Q_c$ is the total rate of sensible heat transfer from the airstream to the pellet by conduction and convection (considered negative), $Q_{es}$ is the total rate of heat transfer to the pellet due to the sublimation of water vapor onto the dry ice (considered negative), $Q_s$ is the heat absorbed by the pellet due to the sublimation of the dry ice itself (considered positive), $Q_r$ is the net heat transfer due to radiation (considered negative), and $Q_d$ is the sensible and latent heat released due to the cooling and freezing of impacting water droplets (considered negative).

End effects are ignored in the current version of the model. That is to say, sublimation is assumed to occur from the cylindrical surface only and not from the ends of the pellet. Furthermore, it is assumed that the sublimation takes place uniformly both around the circumference and along the length of the cylinder. Thus the pellet, in the model,

retains its cylindrical shape and a constant length as it sublimates. In order to strictly satisfy the cylindrical shape preservation assumption, the pellet would have to rotate about its longitudinal axis.

The individual terms of equation 1 are described as follows:

The total sensible heat transfer from the airstream to the cylindrical surface by conduction and convection is given by:

$$Q_c = \pi DLh(t_s - t_a) \qquad (2)$$

where D is the cylinder diameter, L its length, h is the heat transfer coefficient, and $t_s$ and $t_a$ are, respectively, the pellet surface temperature and the airstream temperature. In the present work, the pellet surface temperature is taken to be -100 C (Fukuta, et al. 1971).

The heat transfer coefficient h is related to the Nusselt number Nu via the definition:

$$h = \frac{k_a Nu}{D} \qquad (3)$$

where $k_a$ is the thermal conductivity of air at the ambient temperature, D is the cylinder diameter and Nu is the Nusselt number.

The Nusselt number was calculated using an expression given by Zukauskas (1972) for smooth circular cylinders in a cross flow of air:

$$Nu = 0.26\ Re^{0.6} \qquad (4)$$

This expression is valid over the range $10^3 \leq Re \leq 10^5$. which includes the Re range of practical interest. An alternate method, using the results from the wind tunnel experiments to determine a relation between the

Nusselt and Reynolds numbers was also explored. These results are presented in Appendix A.

The total latent heat transfer due to sublimation of the water vapor onto the dry ice is given by (Lozowski et al.; 1979):

$$Q_{es} = -\pi DLh\left(\frac{Pr}{Sc}\right)^{.63} \frac{\varepsilon l_s}{Pc_p}\left(e_a(t_a)-e_s(t_s)\right) \qquad (5)$$

where $Pr$ is the Prandtl number of air, $Sc$ is the Schmidt number for water vapor in air, $\varepsilon$ is the ratio of the molecular weights of water vapor and dry air, $l_s$ is the specific latent heat of sublimation of water at the surface temperature, $P$ is the static pressure in the free stream, $c_p$ is the specific heat capacity of dry air at constant pressure, $e_a(t_a)$ is the saturation vapor pressure of water vapor in the air, at the ambient temperature, and $e_s(t_s)$ is the saturation vapor pressure of water vapor at the surface temperature of the pellet.

The saturation vapor pressure of water vapor at the surface temperature is so much less than the saturation vapor pressure at the ambient temperature, that it can be neglected and is assumed to be zero. The derivation of this expression is presented in Appendix B.

The rate of consumption of latent heat required to give rise to a sublimation rate $dm/dt$ (assumed negative) is given by:

$$Q_s = -L_s \frac{dm}{dt} \qquad (6)$$

where $m$ is the mass of the dry ice pellet, and $L_s$ is the specific latent heat of sublimation of dry ice at the surface temperature.

The heat transfer due to radiation is given by:

$$Q_r = -\sigma(T_a^4 \varepsilon_a - T_s^4 \varepsilon_s)\ \pi DL \qquad (7)$$

where $\sigma$ is the Stefan-Boltzmann constant, and $\varepsilon_a$ and $\varepsilon_s$ are the emissivities of the surrounding air and the pellet surface.

The heat transfer by the water droplets can be considered as a three stage process: the heat needed to cool the water droplets to $0^0$ C, the heat needed to freeze the droplets at $0^0$C, and the heat needed to cool the frozen droplets to the pellet surface temperature. This can be expressed as:

$$Q_d = -(c_w R_w(t_a - 0^0C) + R_w L_f + c_i R_w(0^0C - t_s)) \qquad (8)$$

where $c_w$ is the average specific heat capacity of water between $t_a$ and $0^0$C, $R_w$ is the mass flux of droplets collected per unit time, $L_f$ is the specific latent heat of freezing at $0^0$C, and $c_i$ is the average specific heat capaoity of ice between $0^0$C and $t_s$.

The contributions to the heat balance due to the water droplets and radiation have been neglected in the model. The justification is found in Appendix C.

Substituting expressions (2), (5), and (6) into equation (1) yields:

$$\frac{dm}{dt} = \frac{\pi DLh}{L_\delta}\left[(t_s - t_a) - \left(\frac{Pr}{Sc}\right)^{.63} \frac{\varepsilon l_s}{Pc_p} e_a(t_a)\right] \qquad (9)$$

Substituting equation (3) into (9), expressing the mass as $\pi D^2 L\rho_c/4$, where $\rho_c$ is the dry ice pellet density (experimentally determined to be 1.4 $gcm^{-3}$) and taking to be constant we obtain the following relationship:

$$\frac{dD}{dt} = \frac{2k_a Nu}{\rho_c L_\delta D}\left[(t_s - t_a) - \left(\frac{Pr}{Sc}\right)^{.63} \frac{\varepsilon l_s}{Pc_p} e_a(t_a)\right] \qquad (10)$$

An analytic solution to this relationship exists when the ambient conditions (temperature and wind speed) can be held constant like in a wind tunnel. The solution is presented in Appendix D. However, a numerical technique was used to solve this relationship since the numerical model was also going to be used in simulating the free-fall experiments where conditions are not constant. Comparisons were made between the numerical solutions and the analytic solutions. The results were within 5%-10% of each other.

The effect of relative humidity on the sublimation rate can be investigated by substituting the actual vapor pressure (the saturation vapor pressure multiplied by the relative humidity) for the saturation vapor pressure in equation 10. Measurements of the relative humidity within the test section both with the sprays off and on were unfortunately never made. Consequently, the actual vapor pressure in the test section was not known. However, when the sprays were on the relative humidity was assumed to be 100%. Thus the $Q_{es}$ term was retained in cloudy conditions, but it was ignored in clear air.

## 2.2 Sensitivity Tests

The most common way of numerically solving a differential equation is to find an approximate expression for the derivative appearing in the equation. These approximate expressions are formed using differences of the dependent variables over finite space and time intervals. This approach is called the finite difference method, and the resulting algebraic equation is called a finite difference scheme to that differential equation.

A forward differencing finite difference scheme was used to solve equation 10. The model was run varying the time interval to check the numerical accuracy of the solution. The experimental conditions used were $T = -10°C$, $V = 14 ms^{-1}$, and time intervals of 10, 5, 2, 1, 0.5, and 0.25 sec. The results of these experiments are tabulated and appear in Table 1.

| | Δt=0.25sec | Δt=0.5sec | Δt=1sec | Δt=2sec | Δt=5sec | Δt=10sec |
|---|---|---|---|---|---|---|
| Time (sec) | DIAMETER (cm) | | | | | |
| 0 | 1.5 | 1.5 | 1.5 | 1.5 | 1.5 | 1.5 |
| 60 | 1.361454 | 1.361514 | 1.361562 | 1.361621 | 1.361766 | 1.361994 |
| 120 | 1.217016 | 1.217147 | 1.217250 | 1.217377 | 1.217700 | 1.218212 |
| 180 | 1.065357 | 1.065560 | 1.065732 | 1.065948 | 1.066501 | 1.067381 |
| 240 | 0.904547 | 0.904809 | 0.905050 | 0.905377 | 0.906239 | 0.907621 |
| 300 | 0.731349 | 0.731670 | 0.731997 | 0.732481 | 0.733798 | 0.735919 |
| 360 | 0.539680 | 0.540097 | 0.540572 | 0.541323 | 0.543413 | 0.546778 |
| 420 | 0.314613 | 0.315248 | 0.316063 | 0.317439 | 0.321308 | 0.327456 |

Table 1

Sensitivity test results

The results of these tests indicate that the differences in the predicted diameter after 7 minutes are within 4% of each other. As the time step increases from 0.25 sec to 10 sec the error increases only marginally. These tests indicated that the forward differencing finite difference scheme would be adequate, and all subsequent models were run with this scheme, using a time step of 1 second.

# CHAPTER 3

# THE WIND TUNNEL EXPERIMENTS

## 3.1 FROST Tunnel Capabilities

The icing wind tunnel is situated in the Department of Mechanical Engineering and was designed by M. Sroka (1972) and Prof. G. Lock. FROST is an acronym for Fundamental Research on Solidification and Thawing.

A plan view of the icing wind tunnel is shown in Figure 1. The tunnel has an octagonal cross-sectional shape with a diameter of 0.46 m across the flat plates in the working section. The air is impelled through the tunnel by a 22 kW constant speed electric motor direct coupled to a fan. Velocity control is achieved by adjusting a set of vanes immediately downstream of the fan. The air is cooled by a 30 kW refrigerator system. The spray system consists of four pneumatic atomizing nozzles, capable of producing water droplets with diameters typically ranging between 10 $\mu$m to 100 $\mu$m.

The icing wind tunnel is capable of producing air speeds up to 60 $ms^{-1}$ in dry air and 35 $ms^{-1}$ with the sprays on , liquid water contents up to 3 $gm^{-3}$, and temperatures down to -18 °C. The rapid accumulation of ice especially on the turning vanes (Gates, 1981) accounts for the difference in maximum air speed with the sprays on.

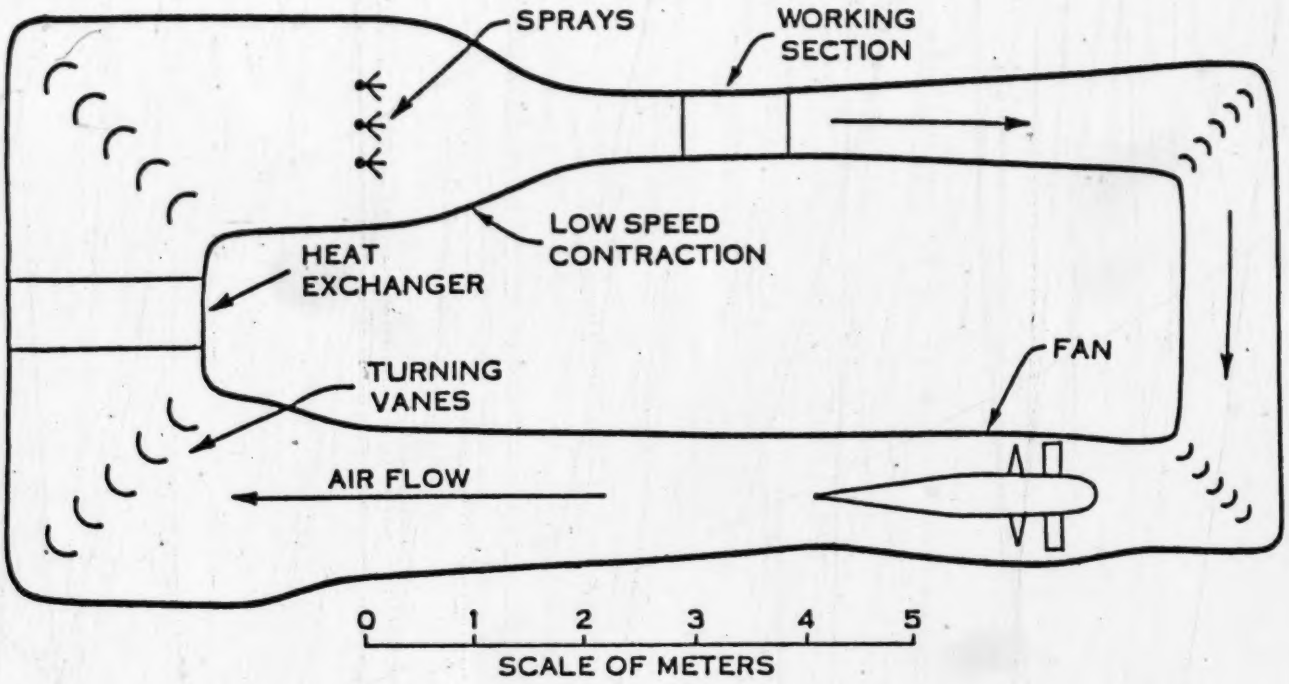


Figure 1

A plan view of the FROST icing wind tunnel.

## 3.2 Experimental Procedure

In the experiments we measured the rate of dry ice sublimation in an airstream. A cylindrical dry ice pellet with a measured diameter and length was suspended by means of an insulated clamp in the center of the 46 cm diameter test section of the tunnel. The cylinder projected at least 5 cm beyond the clamp and was oriented so that its longitudinal axis was perpendicular to the airstream. The airflow was then started and photographs were taken every 10 or 15 seconds looking along the cylinder axis, to document the size and shape change of the cross-section. An ASAHI Pentax camera equipped with a super multi-coated MACRO Takumar 1:4 50mm lens was used to photograph all the experiments. The sublimation was followed to the point where the cylinder became so small that it broke free of the clamp and was swept down the tunnel. Because the cylinder was clamped in a fixed orientation, its cross-section did not remain perfectly circular as it sublimed. In fact, it eventually achieved a wedge shape, as can be seen by the analyzed cross-sections depicted in Figure 2. These results are from experiment 5, conducted at an initial temperature of 18 °C and an airspeed of 14 $ms^{-1}$. The photographs were taken at 10 second intervals. The degree of enlargement is 1.45 the original size.

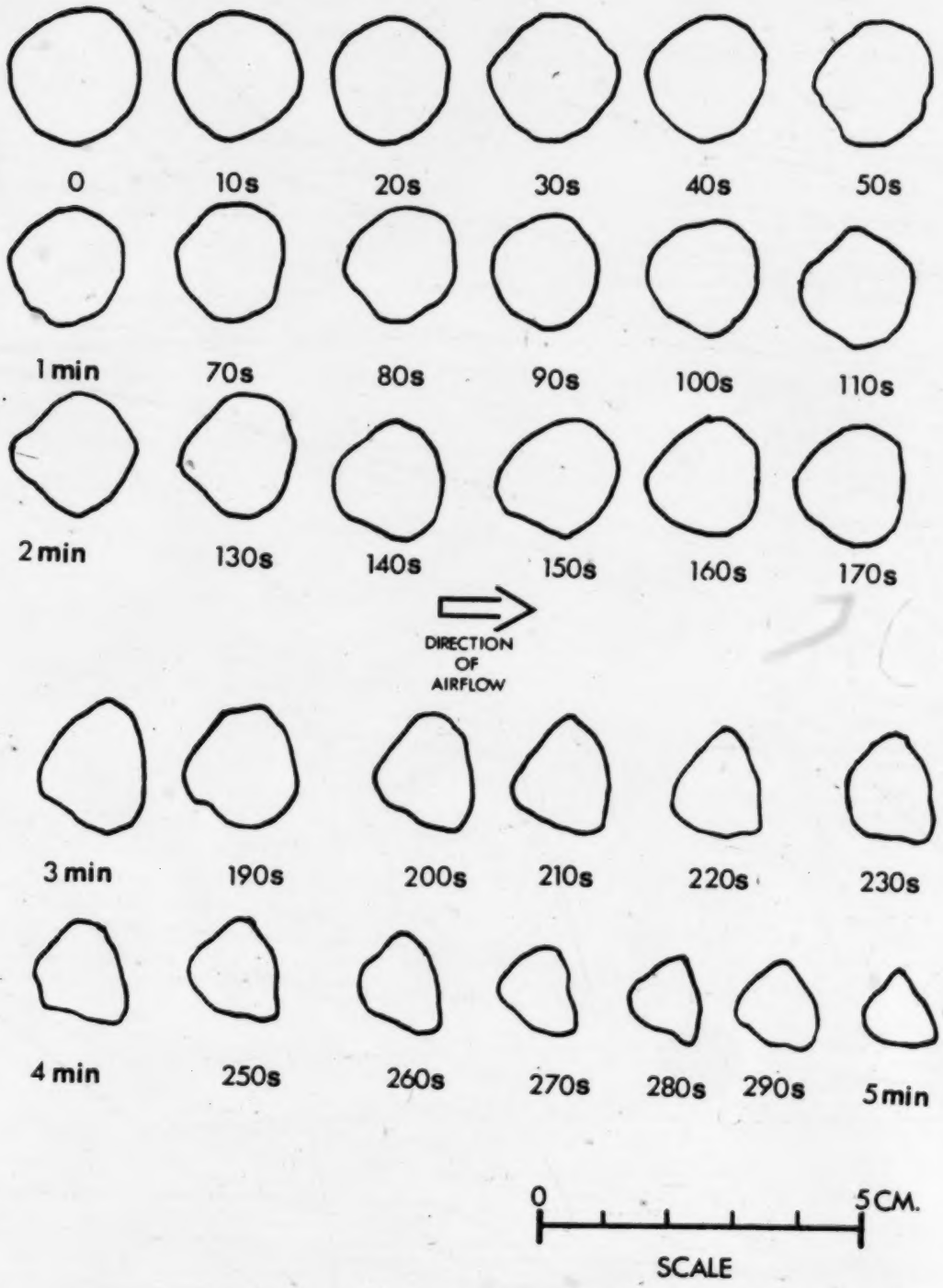


Figure 2

The analyzed cross-sections of a dry ice pellet.

In order to make a comparison with the theory , therefore, the cross-sectional area was measured and an equivalent circular diameter was calculated. Photographs were taken every minute in some of the earlier experiments, to check for changes in length. Subsequent analysis revealed that the lengths did not change by more than 10%, from the original measurement of the length, during the entire duration of the experiment. (As an example; during experiment 10 the diameter changed from 1.40 cm to 0.80 cm after 4 minutes of elapsed time, while the length changed from 7.80 cm to 7.15 cm after 4 minutes)

In order to simulate the sublimation rate of dry ice pellets falling through a cloud, some experiments were conducted in the FROST tunnel with the sprays on. Figure 3 shows the pellet in the working section of the tunnel with the sprays on. The wake of the pellet can be clearly seen.

The measurement of the liquid water content was accomplished by measuring the mass of ice accreted on a rotating cylinder (DeLorenzis, 1980).

The wind speed in the working section was determined by taking observations of the water filled U-tube manometer, which measures the pressure drop across the contraction, and using:

$$\Delta p = 1/2\rho_a V^2 \qquad (11)$$

where $\Delta p$ is the dynamic pressure, $V$ is the airspeed, and $\rho_a$ is the density of air evaluated at the temperature and the pressure (930 mb) of the working section. This formula assumes that the air is

incompressible which may introduce errors that are most likely small since the maximum wind speed was 31 $ms^{-1}$.

The temperature in the working section was measured before and after every experiment using a thermometer. Difficulties in maintaining a constant temperature for the duration of some experiments were due to the heat energy caused by the friction of the airstream on the tunnel walls. A temperature balance is achieved when the frictional heat energy production rate is in equilibrium with the heat transfer through the tunnel walls. This balance at times took longer than the time required to complete a series of experiments.

A total of 32 experiments were conducted in the FROST tunnel varying the temperature and airspeed, and with the sprays on and off. The experimental conditions are summarized in Table 2.

Figure 3

A dry ice pellet suspended in cloudy air, in the FROST tunnel. The wake is clearly visible

| Run No. | Temperature (°C) Before | After | Velocity (in H20) Δp | (ms$^{-1}$) | LWC (gm$^{-3}$) | Time To Breakoff (sec) | Initial Diameter (cm) | Comments |
|---|---|---|---|---|---|---|---|---|
| 1 | 26.5 | 26.5 | 0.10 | 7 | 0 | 40 | 1.27 | |
| 2 | 26.5 | 26.5 | 0.40 | 14 | 0 | 70 | 1.27 | photos every 10 s |
| 3 | 26.5 | 26.5 | 1.70 | 28 | 0 | 100 | 1.27 | |
| 4 | 18.0 | 18.0 | 0.43 | 14 | 0 | 228 | 1.48 | |
| 5 | 18.0 | 19.5 | 0.45 | 14 | 0 | 300 | 1.54 | photos every 10 s |
| 6 | 19.5 | 19.5 | 0.43 | 14 | — | 290 | 1.53 | |
| 7 | 19.5 | 19.5 | 0.43 | 14 | — | 170 | 1.52 | |
| 8 | -10.0 | -10.0 | 0.40 | 13 | 0 | 362 | 1.54 | |
| 9 | -10.0 | -10.0 | 0.40 | 13 | 0 | 396 | 1.59 | photos every 15 s |
| 10 | -10.0 | -10.0 | 0.40 | 13 | 0.45 | 391 | 1.53 | |
| 11 | -10.0 | -10.0 | 0.40 | 13 | 0.38 | 300 | 1.61 | |
| 12 | -10.0 | -10.0 | 0.40 | 13 | 1.40 | 342 | 1.54 | |
| 13 | -10.0 | -10.0 | 0.40 | 13 | 1.72 | 363 | 1.64 | |
| 14 | -10.0 | -10.0 | 0.40 | 13 | 0 | 308 | 1.43 | |
| 15 | -12.0 | -12.0 | 0.45 | 13 | 0 | 330 | 1.40 | |
| 16 | -12.0 | -12.0 | 0.45 | 13 | 0 | 390 | 1.41 | photos every 15 s |
| 17 | -11.0 | -11.0 | 0.40 | 13 | 0.42 | 420 | 1.36 | |
| 18 | -11.0 | -11.0 | 0.40 | 13 | 0.65 | 402 | 1.35 | |
| 19 | 24.0 | 24.0 | 0.41 | 14 | 0 | 343 | 1.52 | |
| 20 | 32.5 | 32.5 | 0.42 | 14 | 0 | 238 | 1.40 | photos every 15 s |
| 21 | 32.5 | 32.5 | 0.42 | 14 | 0 | 295 | 1.44 | |
| 22 | 32.5 | 32.5 | 0.42 | 14 | 3.08 | 204 | 1.62 | |
| 23 | 32.5 | 32.5 | 0.42 | 14 | 3.08 | 154 | 1.61 | |
| 24 | 34.0 | 34.0 | 0.43 | 14 | 0.46 | 223 | 1.60 | |
| 25 | 34.0 | 34.0 | 0.43 | 14 | 0.46 | 159 | 1.65 | |
| 26 | 27.0 | 30.0 | 0.43 | 14 | 0 | 243 | 1.32 | |
| 27 | 30.0 | 32.0 | 0.52 | 16 | 0 | 247 | 1.39 | |
| 28 | 32.0 | 34.1 | 0.52 | 16 | 0 | 182 | 1.24 | photos every 15 s |
| 29 | 34.1 | 35.5 | 0.52 | 16 | 0 | 112 | 1.62 | for exp 26-30 |
| 30 | 35.5 | 35.5 | 0.52 | 16 | 0 | 240 | 1.54 | |
| 31 | 37.0 | 37.5 | 2.00 | 31 | 0 | 80 | 1.45 | photos every 7.5s |
| 32 | 37.5 | 37.5 | 2.00 | 31 | 0 | 165 | 1.52 | for exp 31-32 |

Table 2

Summary of Experimental Conditions

## 3.3 Experimental Observations at High Temperatures

A total of twenty one experiments were carried out at temperatures above 0 °C. Six of these experiments were conducted with the sprays on, in order to investigate the effect of cloud on the sublimation rate of dry ice. Refrigeration problems experienced after conducting experiments 6 and 7 prevented the measurement of liquid water contents. A rotating clamp was designed for experiments 26 through 32 to eliminate the wedge shapes of the earlier experiments.

The results of the experiments carried out in high temperatures with the sprays off are presented in Figures 4 through 12. The smooth curves represent the model predictions of the change in equivalent circular diameter with time. The jagged lines join the experimental observations obtained from the analysis of the photographs recorded every 7.5, 10 or 15 seconds. The specific time intervals are indicated in Table 2. The temperatures in the working section of the tunnel varied from 18.0 °C to 37.5 °C. Velocities in the tunnel were maintained close to 14 $ms^{-1}$ with some running at 16$ms^{-1}$. Experiments 31 and 32 were conducted at a much higher velocity of 31 $ms^{-1}$ in order to test the response of the model to such extreme conditions.

The differences in the initial pellet diameter, between experiments conducted under the same conditions, sometimes varied by as much as 0.11 cm. Hence, after the photographs were analyzed, the experimental curves were shifted to a common initial diameter, for comparison with the model predictions. This technique also provided additional information on the measurement variability encountered among these experiments.

The model predictions generally were within 10%-15% of the experimental observations . Good agreement was shown for the first 90 to 120 seconds; however, there was a tendency for the model to overpredict the sublimation rate especially at long times. Discrepancies may be due to erroneous estimation of diameter due to rime observed forming on the pellet, which was subsequently blown off. Also the pellets after some time ,would sometimes slip in the clamp and not be perpendicular to the airstream, again giving an over-estimate of the diameter. The shape change from circular to wedge also contributed to the discrepancies. Another possible source of error may be due to the clamp's effect on the air flow pattern around the pellet. The variability in actual pellet density could also be a source of experimental error. Some pellets could be more dense than 1.4 $gcm^{-3}$, and would not sublime as quickly as predicted. A possibility also exists that the model assumption of a dry ice surface temperature of -100 °C (Fukuta, et al.,1971) may be an overestimate. A colder surface would imply a bigger heat flux and hence a faster sublimation rate.

The purpose in using a rotating clamp in the last series of experiments, was to try to eliminate the shape change problem identified in the earlier experiments. This modification did indeed make the analysis of the photographs easier. The variability between experiments is not as great, as seen in Figure 12, in fact the observations were all within 10% of each other. This agreement between experiments could also be attributable to a more uniform sample of dry ice obtained from the manufacturing company.

The results of the experiments carried out in warm temperatures with the sprays on are presented in Figures 13 through 15. Comparisons with the model predictions for the first 2 minutes show reasonably good agreement. The pneumatic atomizing nozzles were not functioning properly during experiment 6, resulting in a poor distribution of the spray in the working section. This may account for the poor agreement with the model predictions. Again a layer of frost was observed forming on the surface of the pellet, possibly accounting for discrepancies in diameters. The results in Figures 14 and 15 suggest that the liquid water content has little effect on the change in diameter.

A direct comparison between the model predictions and experimental observations when the sprays are on and when they are off is difficult to make because the experiments did not begin at the same diameter. However, by shifting the curves to a common diameter a comparison can be made. A decrease of 38% in diameter is predicted after 90 seconds, (Figure 6), by the model when the sprays are off. A decrease of 64% in diameter is predicted after 90 seconds, (Figure 14), by the model when the sprays are on. Thus the effect of the cloud is to enhance the heat transfer and thereby to accelerate the rate of sublimation.

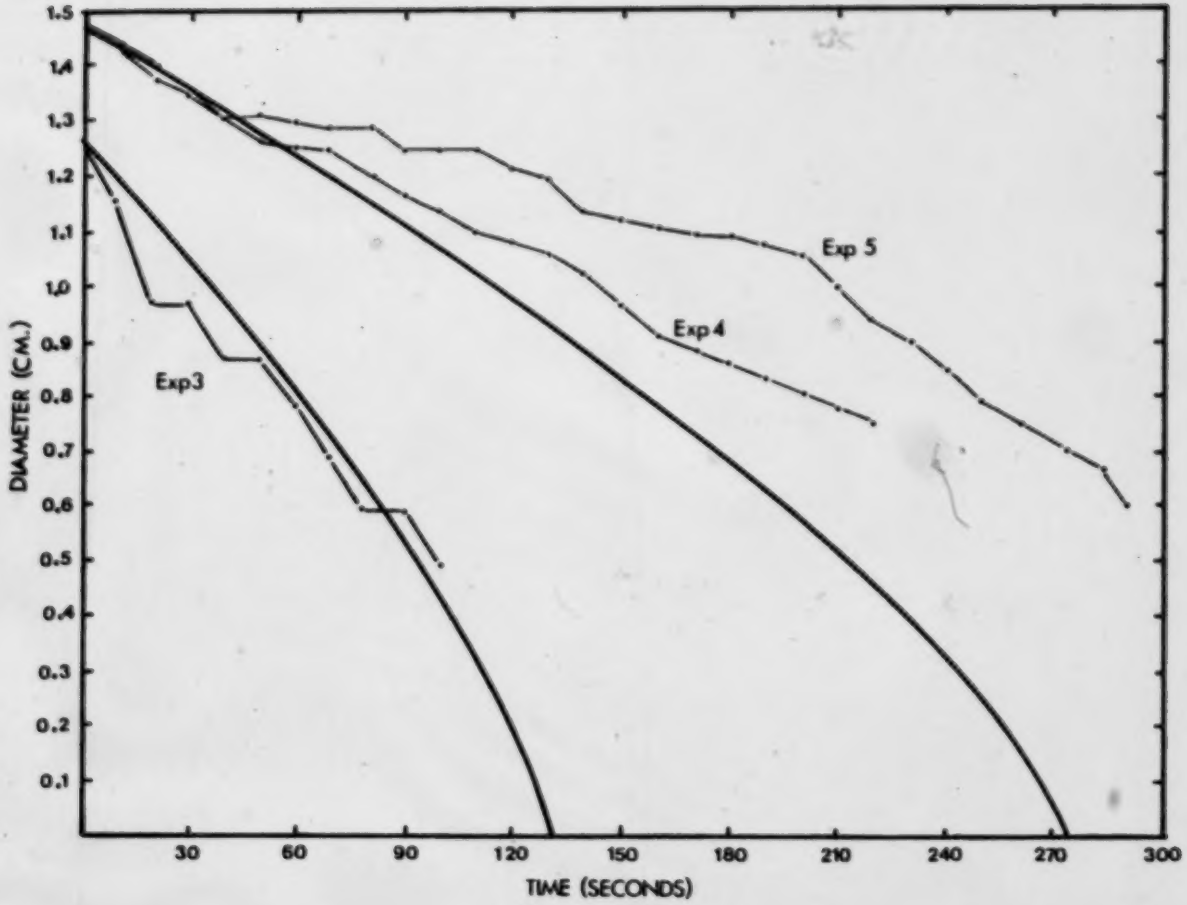


Figure 4

A comparison of theory and experiment at warm temperatures with the sprays off. The heavy lines are the theoretical prediction, and the jagged lines are the experimental observations. The conditions for experiment 3 were: 28 $ms^{-1}$, 26.5 °C. The conditions for experiments 4 and 5 were: 14 $ms^{-1}$; 18.5 °C.

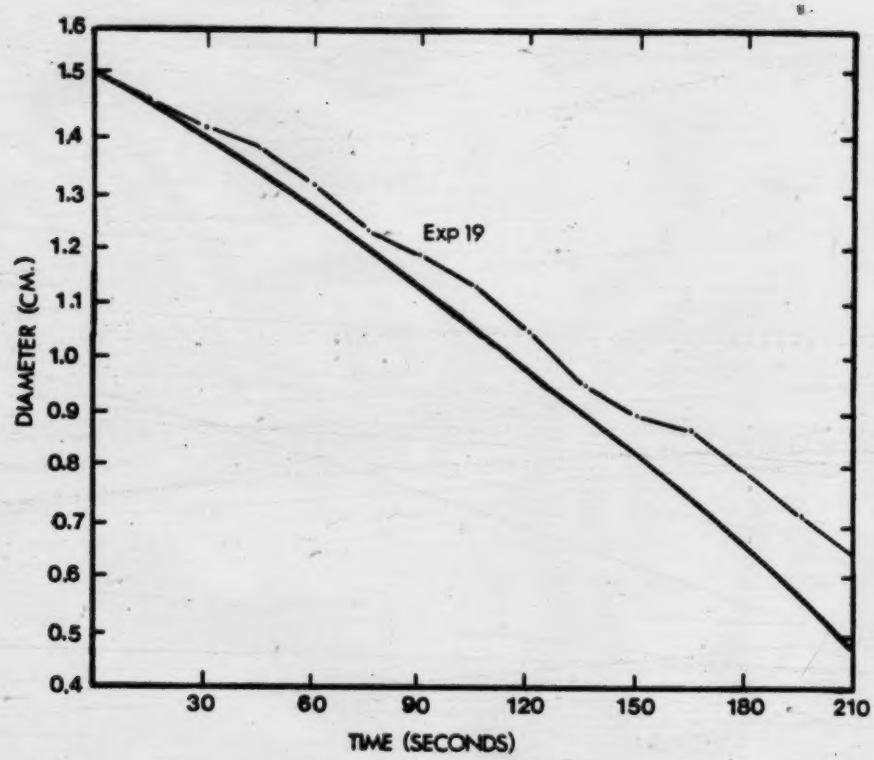


Figure 5

Same as Figure 4. Conditions for experiment 19 were; 14 $ms^{-1}$, 24 °C.

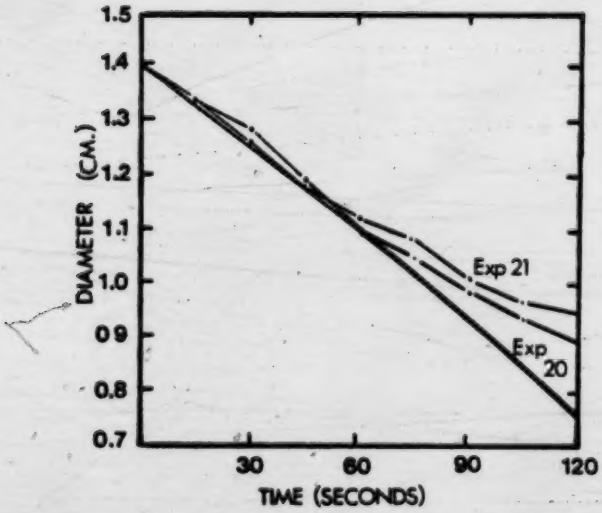


Figure 6

Same as Figure 4. Conditions for experiments 20 and 21 were; 14 $ms^{-1}$, 32.5 °C.

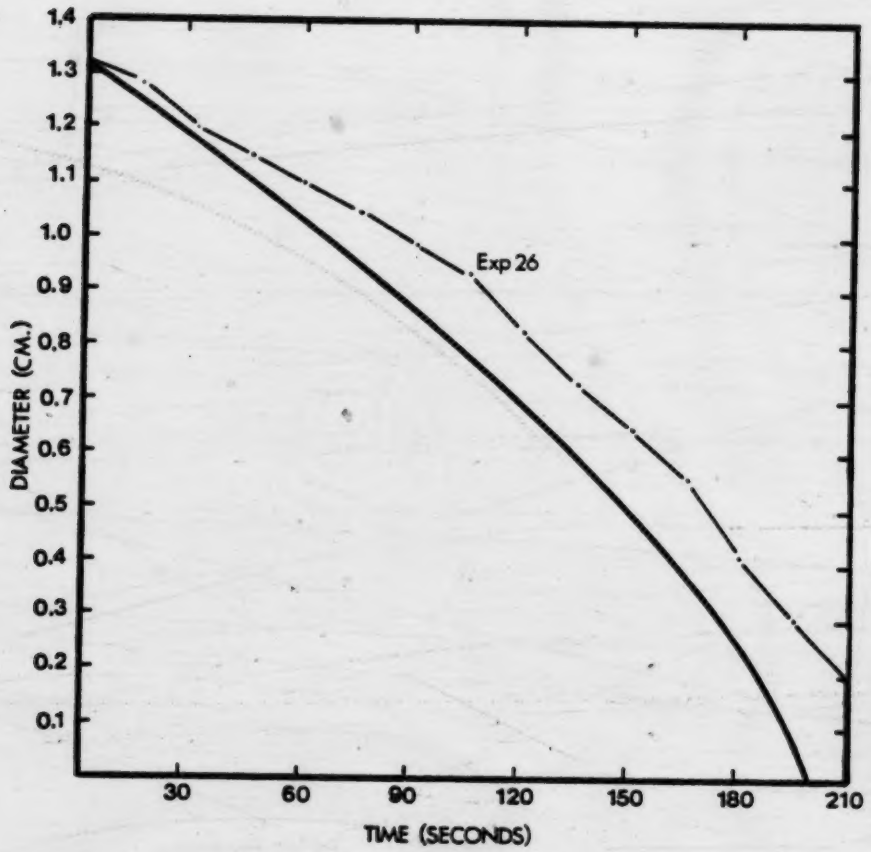


Figure 7

Same as Figure 4. Conditions for experiment 26 were; 14 $ms^{-1}$, 28.5 °C.

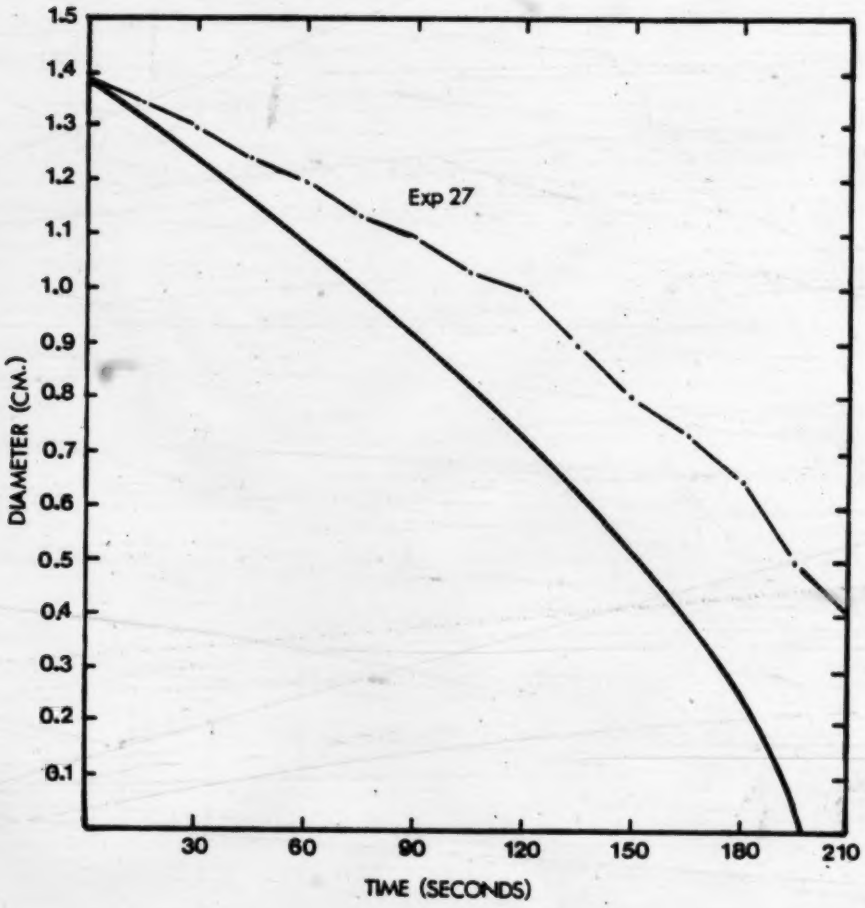


Figure 8

Same as Figure 4. Conditions for experiment 27 were; 16 $ms^{-1}$, 31.0 °C.

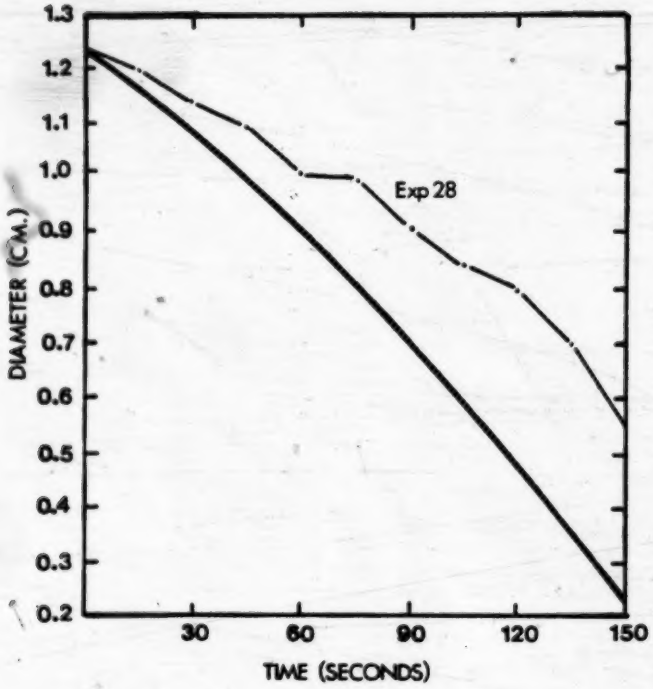


Figure 9

Same as Figure 4. Conditions for experiment 28 were; 16 $ms^{-1}$, 33.0 °C.

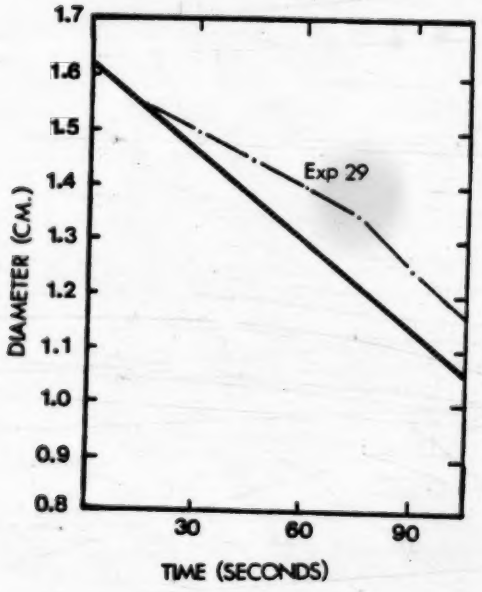


Figure 10

Same as Figure 4. Conditions for experiment 29 were; 16 $ms^{-1}$, 34.6 °C.

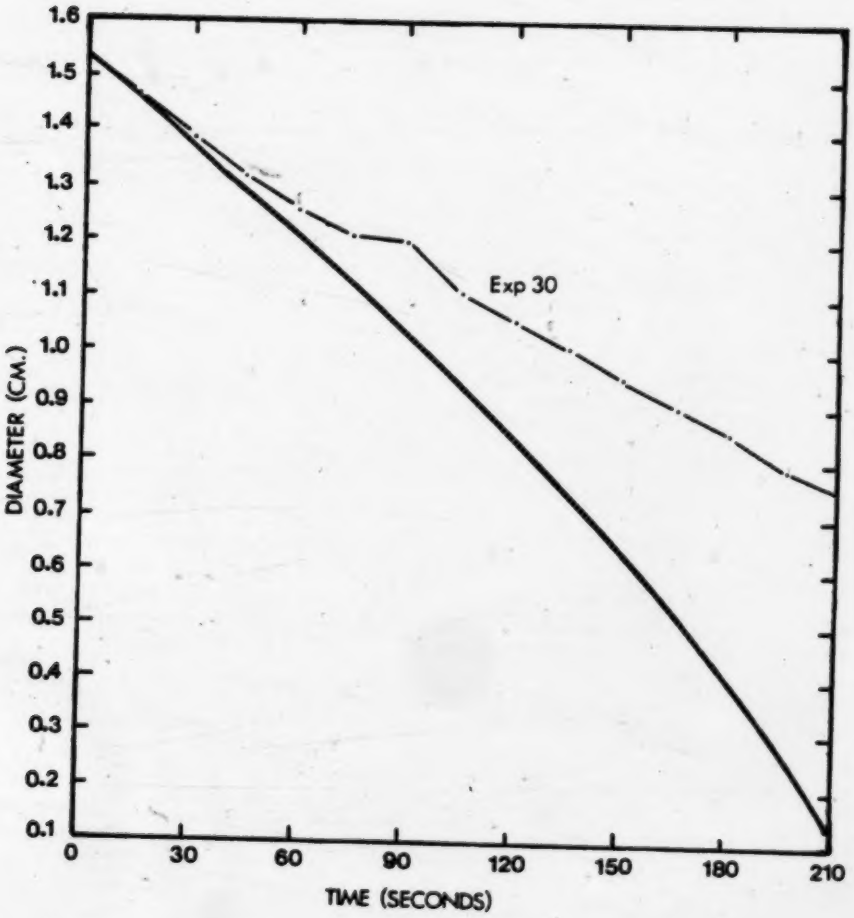


Figure 11

Same as Figure 4. Conditions for experiment 30 were; 16 $ms^{-1}$, 35.5 °C.

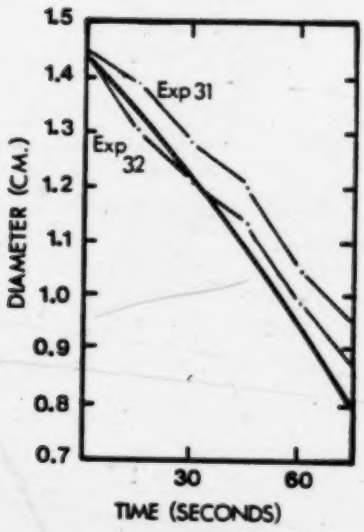


Figure 12

Same as Figure 4. Conditions for experiments 31 and 32 were: 31 $ms^{-1}$, 37.5 °C.

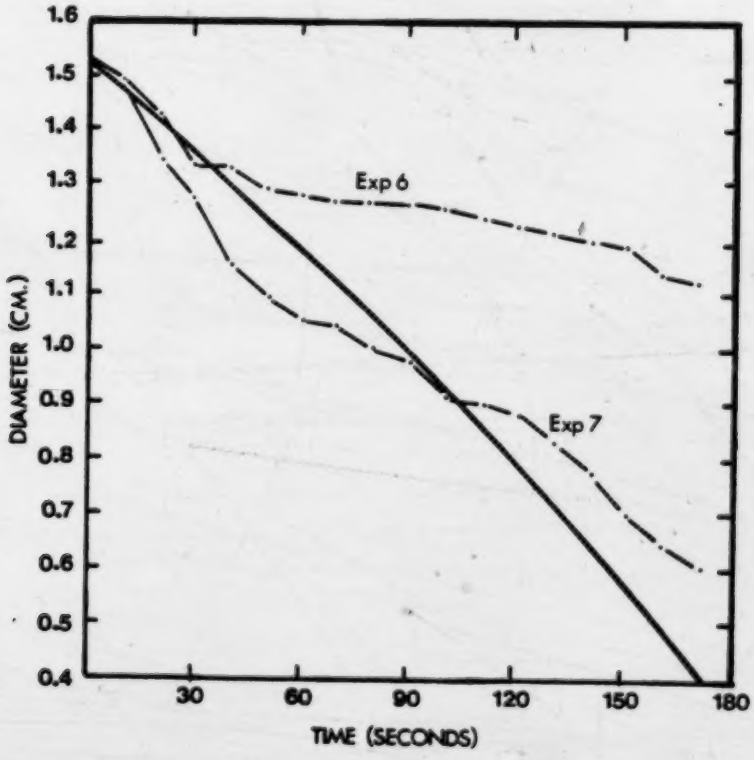


Figure 13

A comparison of theory and experiment at warm temperatures with the sprays on. The heavy lines are the theoretical prediction, and the jagged lines are the experimental results. The conditions for experiments 6 and 7 were: 14 $ms^{-1}$, 19.5 °C. LWC was not available.

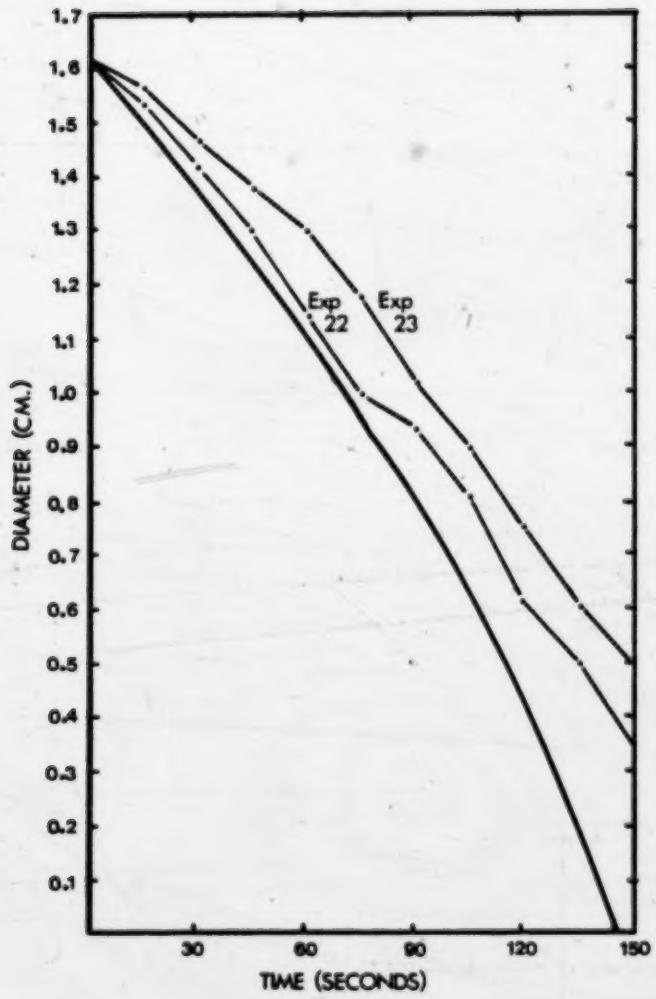


Figure 14

Same as Figure 13. Conditions for experiments 22 and 23 were: 14 $ms^{-1}$, 32.5 °C, 3.08 $gm^{-3}$.

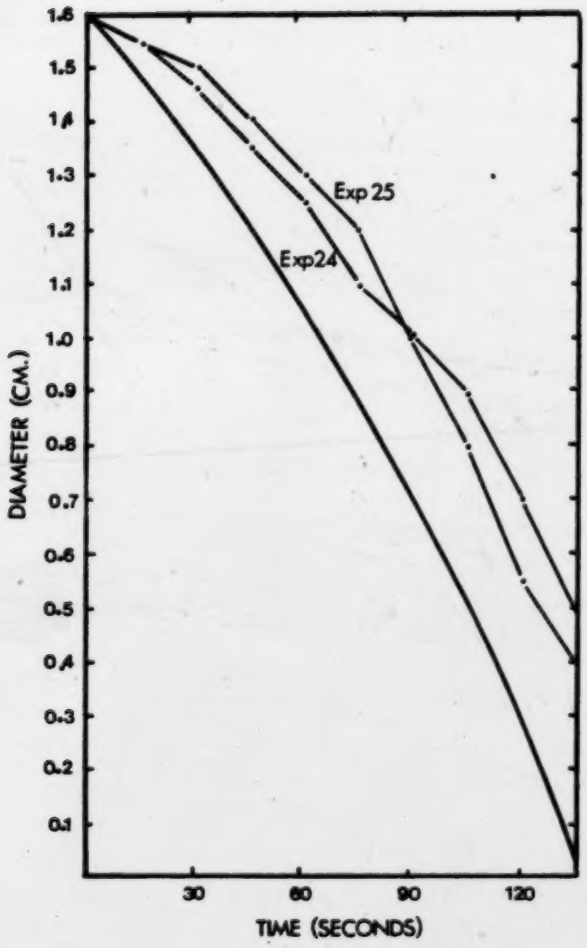


Figure 15

Same as Figure 13. Conditions for experiments 24 and 25 were; 14 $ms^{-1}$, 34.0 °C, 0.46 $gm^{-3}$.

## 3.4 Experimental Observations at Low Temperatures

A total of eleven experiments were carried out at temperatures below 0 °C. Six of these experiments were conducted with the sprays on, in order to investigate the effect of cold clouds on the sublimation rate of dry ice. In all cases photographs were taken every 15 seconds.

The results of experiments conducted at cold temperatures with the sprays off are presented in Figures 16 and 17. All these experiments were carried out at an airspeed of 13 $ms^{-1}$, and temperatures of −10 °C or −12 °C. The sublimation of the pellets is expected to take longer, since the temperature gradient between the environment and the pellet surface is not as steep as when the environmental temperature is above 0 °C. The model predictions show very good agreement with the experimental observations. The tendency for the model to overpredict the sublimation rate is not as obvious as in the high temperature cases, but it is still evident.

The effect of ambient temperature on the sublimation rate can best be seen by comparing Figures 6 and 16. Using the shifting curve technique, the model predicts a 10% change in diameter, (Figure 16), after 60 seconds of elapsed time, when the temperature is −10 °C and the airspeed is 13 $ms^{-1}$. When the temperature is 32.5 °C and the airspeed is similar, the model predicts a 21% change in diameter, (Figure 6), after 60 seconds of run time.

The results of experiments carried out at cold temperatures with the sprays on are presented in Figures 18 and 19. Experiments 10,11,12,and 13 were conducted at an airspeed of 13 $ms^{-1}$, a temperature of −10 °C, and liquid water contents of 0.45 $gm^{-3}$, 0.38 $gm^{-3}$, 1.40 $gm^{-3}$,

and 1.72gm$^{-3}$ respectively. The results of the model are in good agreement with the observations. As the liquid water content increases, the observations show a decrease in the diameter, but they are all within 10% of the model prediction, suggesting that the liquid water has little effect on the sublimation rate. A decrease of 14.2% in the diameter after 90 seconds, (Figure 16) is predicted by the model when the sprays are off. A decrease of 15.7%, (Figure 18), is predicted by the model when the sprays are on. The inclusion in the model of the deposition of water vapor and its latent heat, when the sprays are on, appears to have little effect on the sublimation rate at low temperatures.

The behaviour of the numerical model under varying conditions is summarized in Figure 20. The ambient temperature has the largest effect on the sublimation rate. The warmer the environmental conditions are, the more rapid the sublimation rate. The effect of a cloudy environment tends to enhance the sublimation rate of dry ice, especially in conditions above 0 °C. The conduction-convection term is the dominant heat transfer process in all cases. The latent heat due to sublimative heating of water vapor is a supporting term which is more important to take into account in warm environments. Its effect in a cold and cloudy environment is almost negligible.

While writing this thesis, it came to my attention that a paper on experimental studies of dry ice nucleation (Horn et al.,1982) was forthcoming. A subsequent telephone conversation revealed that they had questioned the Fukuta surface temperature and used a surface temperature of -78 °C. This assumption was noted earlier in my report as a possible source of error. I therefore, decided to rerun some of the numerical

experiments with a surface temperature of -78 °C.

Results from the 4 different conditions (warm and dry; warm and saturated; cold and dry; cold and saturated) are presented in Figures 21 to 24. The model predicts a slower sublimation rate for all conditions considered. These predictions show better agreement with the experimental observations, confirming the earlier concerns about the surface temperature.

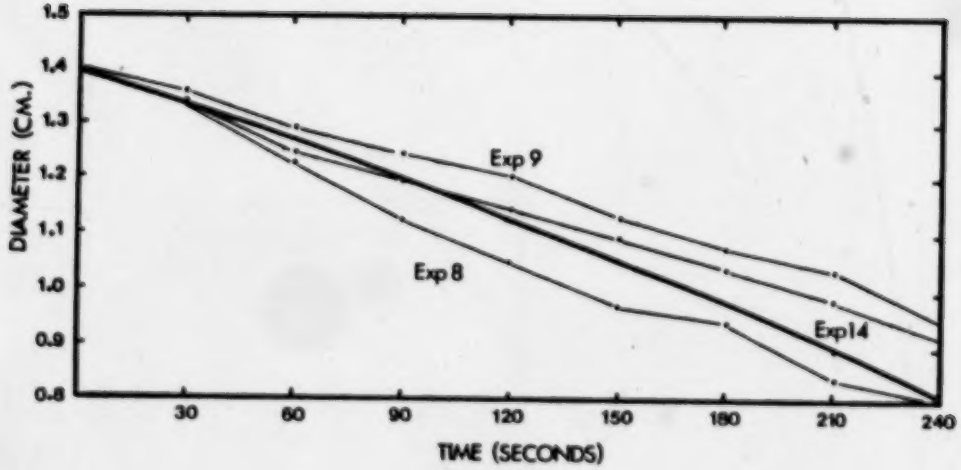


Figure 16

A comparison of theory and experiment at cold temperatures with the sprays off. The heavy lines are the theoretical prediction, and the jagged lines are the experimental observations. The conditions for experiments 8, 9 and 14 were: 13 $ms^{-1}$, -10.0 $^{o}C$.

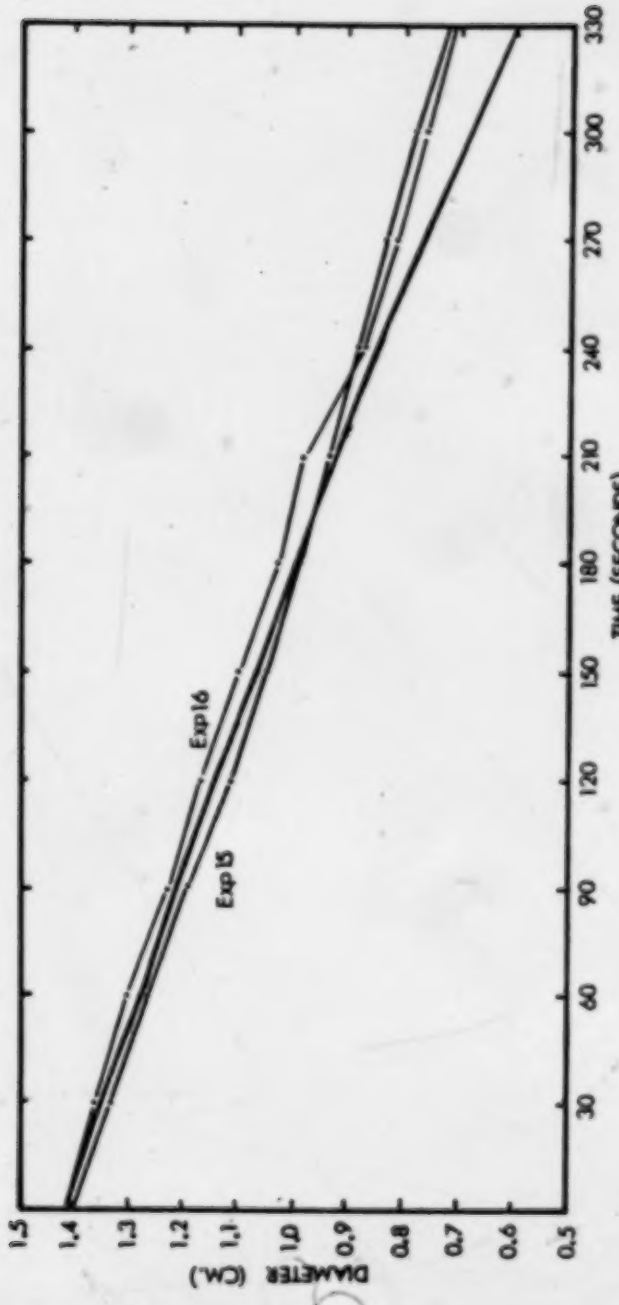


Figure 17

Same as Figure 16. Conditions for experiments 15 and 16 were: 13 $ms^{-1}$, -11.0 °C.

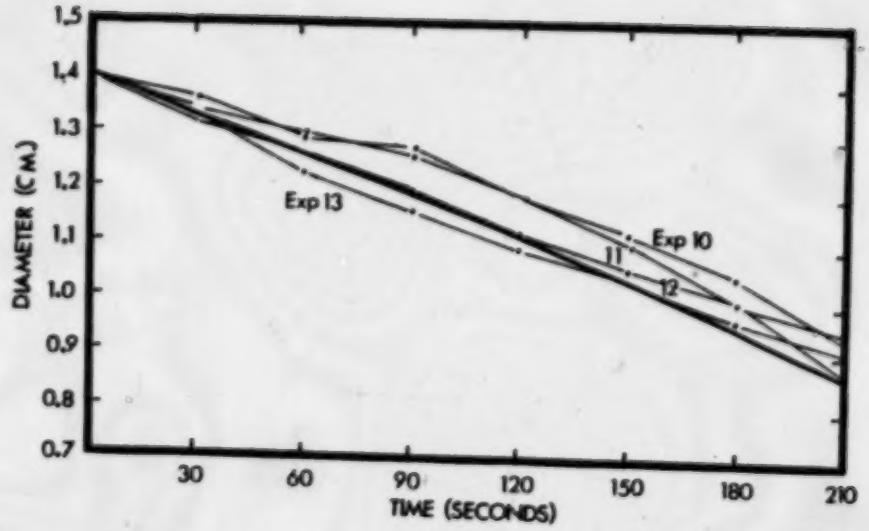


Figure 18

A comparison of theory and experiment at cold temperatures with the sprays on. The heavy lines are the theoretical prediction, and the jagged lines are the experimental observations. The conditions for experiments 10, 11, 12 and 13 were: 13 $ms^{-1}$, -10.0 °C, 0.45 $gm^{-3}$, 0.38 $gm^{-3}$, 1.40 $gm^{-3}$, and 1.72 $gm^{-3}$, respectively.

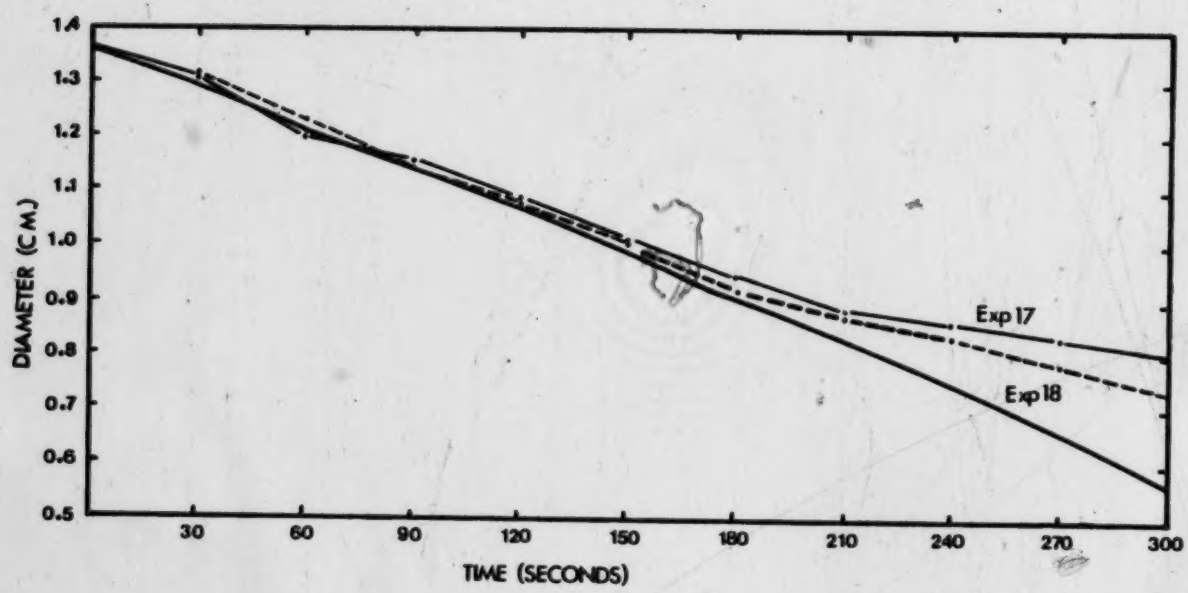


Figure 19

Same as Figure 18. Conditions for experiments 17 and 18 were: 13 $ms^{-1}$, -11.0 °C ,0.42 $gm^{-3}$, and 0.65 $gm^{-3}$, respectively.

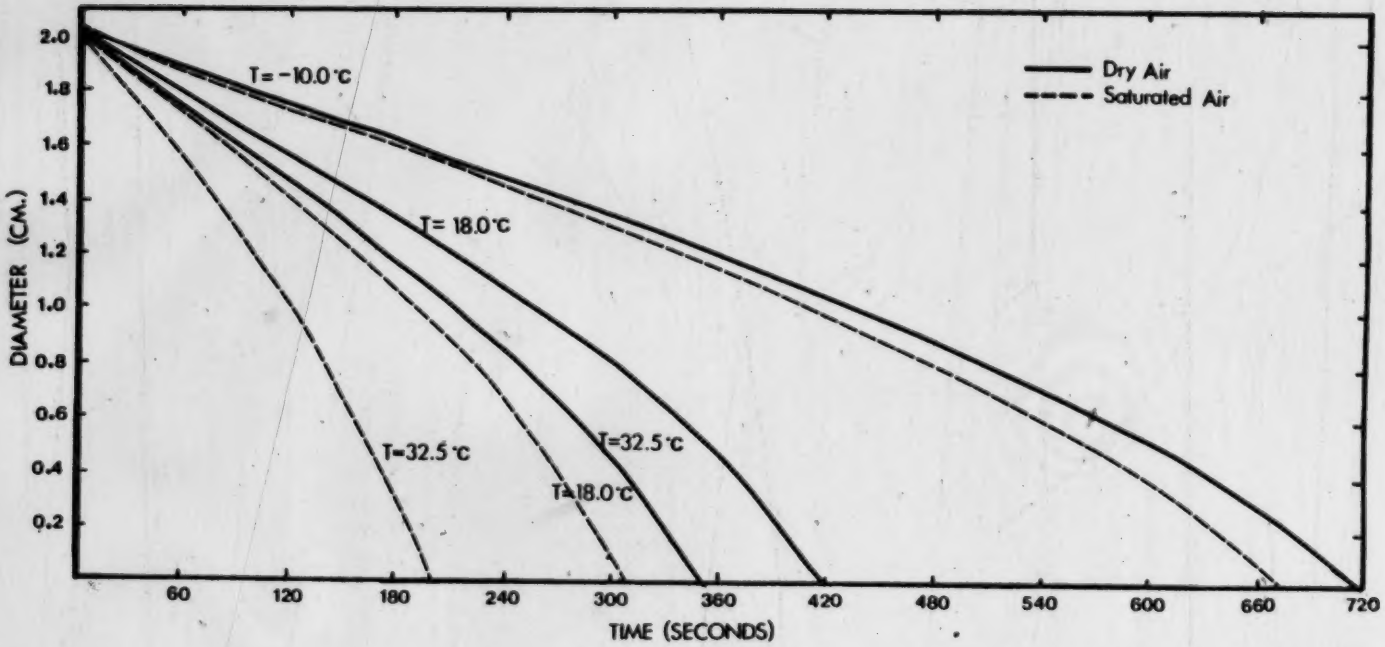


Figure 20

Summary of Theoretical model. The solid line represents a dry environment. The dashed line represents a cloudy environment. All cases were run using a velocity of 14 $ms^{-1}$

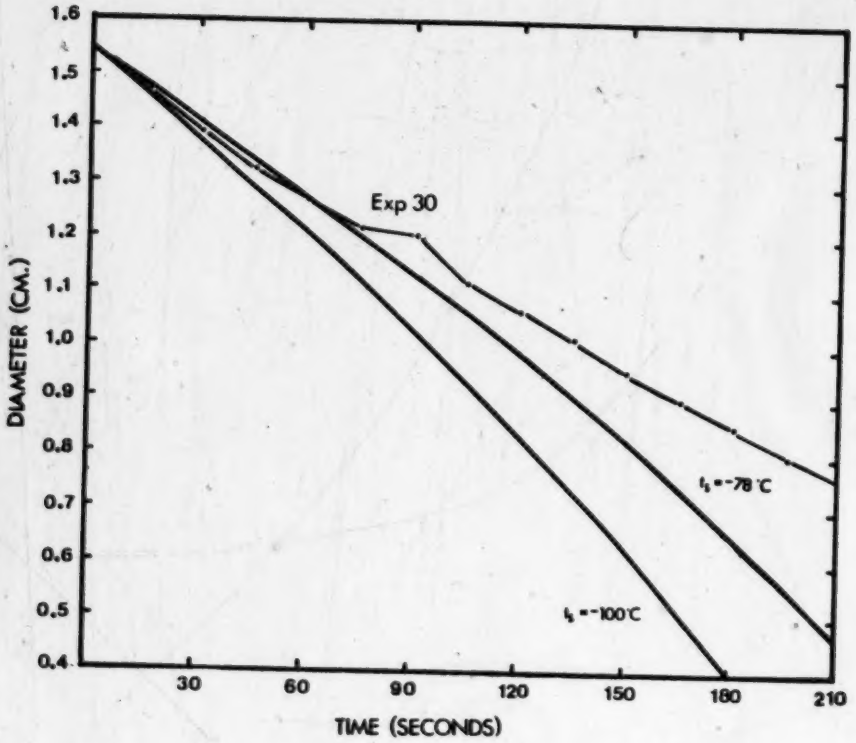


Figure 21

Same as Figure 11. Theoretical prediction determined using a dry ice surface temperature of $-78^{\circ}C$.

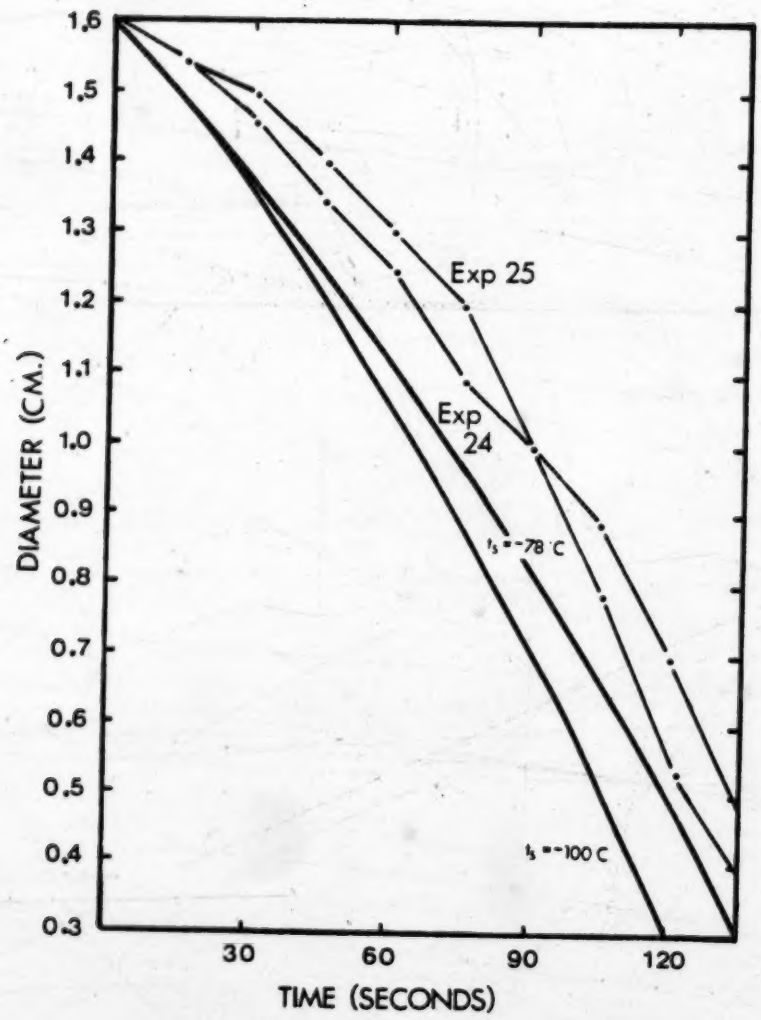


Figure 22

Same as Figure 15. Theoretical prediction determined using a dry ice surface temperature of -78°C.

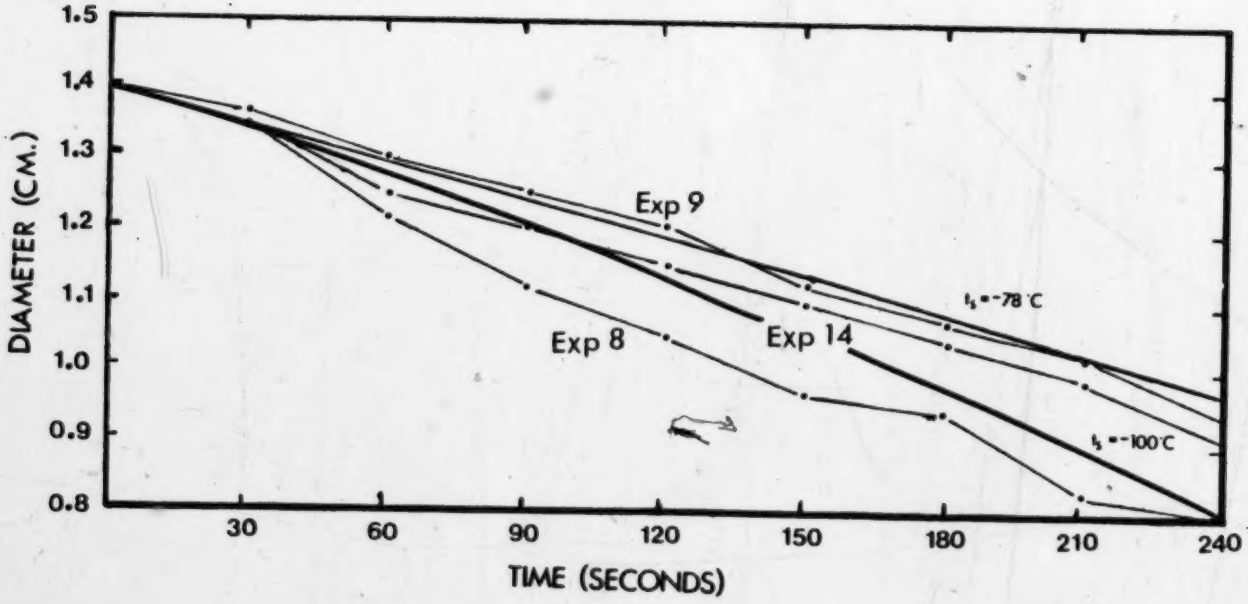


Figure 23

Same as Figure 16. Theoretical prediction determined using a dry ice surface temperature of -78°C.

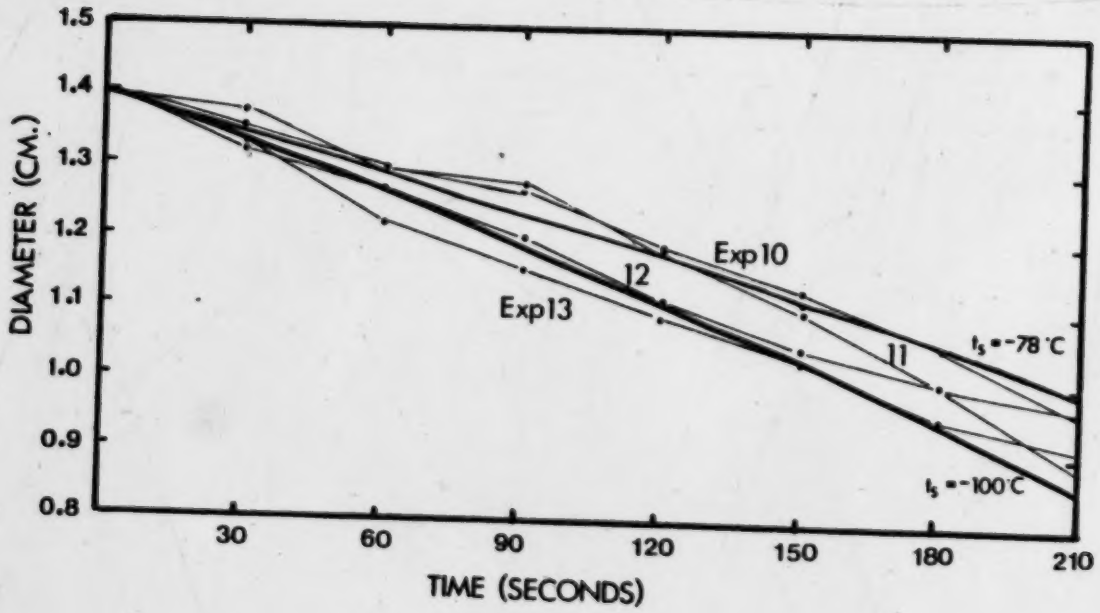


Figure 24

Same as Figure 18. Theoretical prediction determined using a dry ice surface temperature of -78°C.

# CHAPTER 4

# THE FREE-FALL EXPERIMENTS

## 4.1 Free-Fall Model Description

The theory developed in Chapter 2, was incorporated into a free-fall model. In comparing the predictions of equation 10 with the wind tunnel experiments, the wind speed which enters Re and Nu is taken to be a constant. However, for calculating sublimation during free-fall, the wind speed must be the pellet's terminal velocity.

An object or body in free fall attains its terminal velocity when the drag and buoyancy forces are balanced by the gravitational force. The development of the expression for the terminal velocity of a cylindrical object falling freely in air, in a horizontal orientation, is given in Appendix E. The terminal velocity is given by:

$$V_T = \left(\frac{\pi \rho_c g D}{2 C_D \rho_a}\right)^{1/2} \qquad (12)$$

where $g$ is the acceleration due to gravity, $\rho_a$ is the air density and $C_D$ is the drag coefficient of the cylinder.

Drag coefficients for objects of given shapes depend primarily on the Reynolds number. The drag coefficients for circular cylinders of several different aspect ratios are presented in the following table. All the values of $C_D$ are valid in the Reynolds range of $10^3 \leq Re \leq 10^5$, (Hoerner, 1965).

| Aspect Ratio L/d | Drag coefficient | Reynolds No. range |
|---|---|---|
| 1 | 0.63 | $10^3 \leq Re \leq 10^5$ |
| 5 | 0.80 | |
| 10 | 0.83 | |
| 20 | 0.93 | |
| 30 | 1.0 | |
| $\infty$ | 1.2 | |

Table 3

The Drag Coefficient of Truncated Circular Cylinders

A drag coefficient value of 0.8, corresponding to an aspect ratio of 5 was used in the free-fall model. An atmospheric lapse rate of 6.6 $^{o}Ckm^{-1}$ was used in order to specify the variation of the ambient air temperature with height during the fall of the pellet. The change in the aspect ratio due to sublimation was ignored.

## 4.2 The Free-Fall Experiments

A series of free-fall experiments was conducted, in which cylindrical dry ice pellets were dropped from an aircraft flying at 305 m, 460 m, and 610 m above an unused runway (915 m MSL). The intention was to measure the time taken for the cylindrical pellets to reach the

ground, and the final diameters they achieved, and to compare these with the free-fall model predictions.

Prior to the drops, plastic bags with about 1-2 kg of pellets (cylinders with average diameters of 1.27 cm, varying between 1.2-1.5 cm, and average lengths of 5.0 cm, varying between 1.3-6.8 cm), were prepared. As the aircraft approached the runway, the contents of a bag were dropped through an opening in the bottom of the plane. An observer on the ground followed the aircraft through a pair of binoculars, and timed the fall of the pellets with a stop watch.

The model predictions of the time taken for the pellets to reach the ground, and the final diameters they would achieve are presented in Figure 25. The solid lines show the pellet diameter as a function of height, for the three different release heights. Superimposed on these lines are isochrones, in seconds, represented by the dashed lines. For pellets of initial diameter 1.50 cm, the predicted fall times for the three release heights are 15.7, 23.4, and 30.1 seconds, respectively, with corresponding final diameters of 1.42, 1.40, and 1.34 cm. The observed fall times for the first pellets reaching the ground were 18, 26, and 36 seconds.

The difference between the predicted and observed fall times could arise if the pellets encounter thermals as they fall, thereby retarding their fall. Another reason for the difference could be that the drag coefficient on the pellets is somewhat larger than the value 0.8 considered in the model prediction. If a higher value of the drag coefficient was used, the model would then predict fall times closer to the observed fall times. There appears to be a larger discrepancy

between the predicted and observed fall times as the release height is increased. Scintillations observed through binoculars as the pellets fell suggest that tumbling of some sort was most probably occuring. The pellets in this case would achieve a higher velocity than they would with the longitudinal axis horizontal.

An attempt to compare final diameters between model and experiment was not successful. The pellets dispersed considerably in the horizontal as they fell, (also possibly indicative of tumbling) and many were lost in the tall grass bordering the runway. The next time such experiments are attempted, it would be advantageous to find an area with grass that has been cut. Those that were found on the runway were very much smaller than the predicted sizes. It is suspected that the impact at about 17 $ms^{-1}$, on a hard runway surface probably shattered the pellets, rendering invalid any final comparison of diameters. An experiment was conducted to determine if such was the case. Some dry ice pellets were dropped off the roof of a building (height of 15 m). The impact at about 7 $ms^{-1}$ on the pavement below, indeed shattered the pellets.

## 4.3 A Free Fall Simulation

A series of numerical experiments were conducted by using the model described in section 4.1. This simulation was conducted to determine the amount of dry ice that sublimes within the supercooled region of a cloud.

Dry ice pellets with initial diameters varying from 0.4 cm to 1.0 cm were introduced at the -10°C level. The simulation also assumed an atmosphere with no vertical motions. The results of these numerical experiments are presented in Figure 26. The solid lines are the pellet diameter as a function of height or temperature. The dashed lines represent isochrones in seconds. The results indicate that pellets with diameters between 0.5 cm and 0.6 cm are suggested for efficient use of dry ice when dropped from the -10 °C level. The term 'efficient' means the optimum size of dry ice pellet that will sublime within the supercooled region of a cloud.

The dry ice pellets would have a longer residence time in the supercooled region of a cloud with updrafts. In fact, they might completely sublime above the 0 °C level in a cloud with a vigourous updraft, indicating that larger diameters would be required.

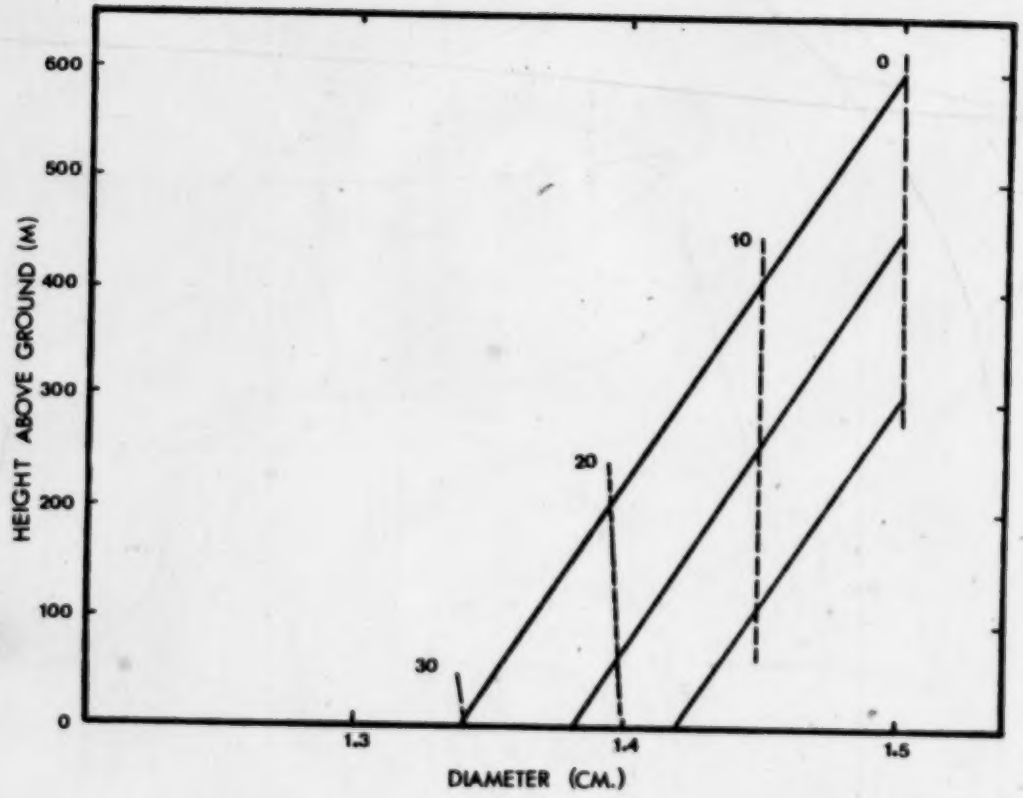


Figure 25
Model predictions for the free-fall experiments. The solid lines are the pellet diameter as a function of height for three release heights. The dashed lines are the isochrones in seconds.

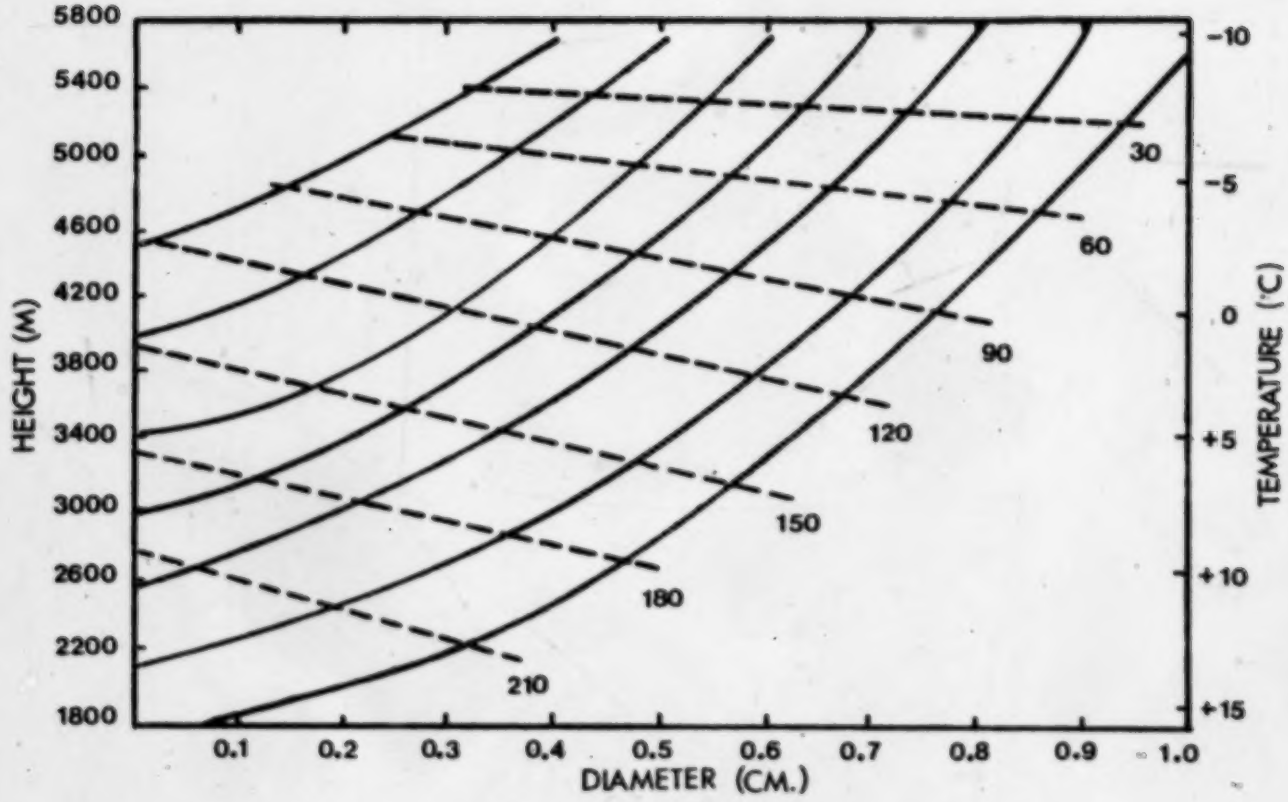


Figure 26

A simulation of dry ice seeding. The solid lines are the pellet diameter as a function of height or temperature. The dashed lines are isochrones in seconds.

# CHAPTER 5

## SUMMARY CONCLUSIONS AND RECOMMENDATIONS

The objective of this thesis was to utilize both heat transfer theory and experimental observation in order to examine the sublimation rate of cylindrical dry ice pellets in clear air and simulated cloud.

A numerical model assuming a heat flux balance at the surface of a cylindrical dry ice pellet was developed. The sublimation was assumed to occur from the cylindrical surface only and not from the ends of the pellet. It was also assumed that the sublimation took place uniformly both around the circumference and along the length of the cylinder, so as to retain its cylindrical shape. The airstream was assumed saturated when simulating a cloud, and was perfectly dry at all other times. The contribution of cloud droplets to the heat transfer was ignored.

A series of thirty two laboratory experiments were conducted in the University of Alberta's FROST icing-wind tunnel facility, to test the theoretical model. These experiments were carried out in both cold and warm environments. Some of the experiments were carried out with the sprays on in order to determine whether a simulated 'cloudy' environment had any effect on the sublimation rate.

The ambient temperature was found to have the largest effect on the sublimation rate of the dry ice pellets. The warmer the environmental conditions, the more rapid was the sublimation rate. The effect of a saturated environment also enhanced the sublimation rate. This effect was more pronounced at warm temperatures, and almost negligible at cold temperatures. In spite of the use of several simplifying assumptions, the cylindrical model, (using a surface temperature of -78°C), predicted

the sublimation rates of dry ice pellets to within 10%, when compared with wind tunnel observations. The model did not perform as well using Fukuta's estimate of the surface temperature of -100 °C.

The theoretical model was then modified to numerically simulate the sublimation rate of cylindrical dry ice pellets in free-fall. A series of nine field experiments was carried out whereby dry ice was released from an aircraft flying at specified altitudes, to verify the model predictions of fall times and final diameters at the ground.

The model predictions of the fall times were within 10-15% of the observed times. Attempts to compare final diameters with the model predictions were not successful. The impact on the runway surface shattered the pellets rendering invalid any final comparisons of diameter.

A numerical simulation of a dry ice seeding experiment was undertaken, to determine the amount of dry ice that sublimes within the supercooled region of a cloud. The results indicated that pellets with diameters between 0.5 cm and 0.6 cm were suggested for efficient use of dry ice when dropped from the -10 °C level.

The FROST icing wind tunnel was an appropriate facility for conducting the sublimation rate experiments. This facility may also be useful for investigations into ice crystal production rates.

## BIBLIOGRAPHY


Achenbach, E., 1977: The effect of surface roughness on the heat transfer from a circular cylinder to the cross-flow of air. International Journal of Heat and Mass Transfer. Vol 20. p359-369

DeLorenzis, B., 1980: Time-Dependent Behaviour of Ice Accretion on a Non-Rotating Cylinder. Unpublished MSc Thesis, University of Alberta, Department of Geography. 92pp

Dennis, A.S., 1980: Weather Modification by Cloud Seeding. International Geophysics Series. Vol 24. Academic Press. New York. 267pp.

English, M., and J.D. Marwitz, 1981: A Comparison of AgI and CO2 Seeding Effects in Alberta Cumulus Clouds. Journal of Applied Meteorology. Vol 20. p483-495

Fukuta, N., W.A. Schmelling, and L.F. Evans, 1971: Experimental determination of ice nucleation by falling dry-ice pellets. Journal of Applied Meteorology. Vol 10. p1174-1179

Gates, E.M., 1981: FROST Tunnel. Department of Mechanical Engineering, University of Alberta. Departmental Report No.26 14pp

Hess, W.N., 1974: Weather and Climate Modification. John Wiley and Sons Inc. New York. 842 pp.

Holroyd, E.W.III, A.B. Super, and B.H. Silverman, 1978: The practicability of dry ice for on-top seeding of convective clouds. Journal of Applied Meteorology. Vol 17. p49-63

Hoerner, S.F., 1965: Fluid Dynamic Drag. Published by the author, 148 Busteed Drive, Midland Park, N.J.,07432, 259pp.

Horn, R.D., W.G. Finnegan, and P.J. DeMott, 1982: Experimental Studies of Nucleation by Dry Ice. Journal of Applied Meteorology. Vol 21. p1567-1570

Huschke, R.E. (ed) 1959: Glossary of Meteorology. American Meteorological Society. Boston, Massachusetts. 638pp

Kopp, F.J., E. Hsie, R.D. Farley, J.H. Hirsch, and H.D. Orville, 1979: Cloud Seeding Simulations. Seventh Conference on Inadvertent and Planned Weather Modification. Banff,Canada. p140-141

List, R., 1963: General heat and mass exchange of spherical hailstones. Journal of the Atmospheric Sciences. Vol 20. p189-197

List, R., P.H. Schuepp, and R.G.J. Methot, 1965: Heat exchange ratios of hailstones in a model cloud and their simulation in a laboratory. Journal of the Atmospheric Sciences. Vol 22. p710-718

Lozowski, E.P., J.R. Stallabrass, and P.F. Hearty, 1979: The icing of an unheated non-rotating cylinder in liquid water droplet-ice crystal clouds. National Research Council of Canada, Division of Mechanical Engineering, Laboratory Technical Report LTR-LT-96.

Lozowski, E.P., and B. Kochtubajda, 1980: Theory and measurements of dry ice sublimation in clear air and simulated cloud. Third International WMO Conference on Weather Modification, Clermont-Ferrand, France. p 409-416

Lowe, P.R., 1977: An approximating polynomial for the computation of saturation vapor pressure. Journal of Applied Meteorology. Vol 16. p100-103

Macklin, W.C., 1963: Heat transfer from hailstones. Quarterly Journal of the Royal Meteorological Society. Vol 89. p319-326

Makkonen, L., 1981: Estimating Intensity of Atmospheric Ice Accretion on Stationary Structures. Journal of Applied Meteorology. Vol 20. p595-600.

Mason, B.J., 1956: On the Melting of Hailstones. Quarterly Journal of the Royal Meteorological Society. Vol 82. p209-216

Mee,T.R.Jr., and W.J. Eadie, 1963: An investigation of specialized whiteout seeding procedures. Research Report 124, U.S.Army CRREL, Hanover, N.H. (NTIS AD414-539/LL)

Mesinger, F., and A. Arakawa, 1976: Numerical Methods Used in Atmospheric Models. Volume 1. GARP Publications Series No. 17 64pp

Morgan, V.T., 1975: The overall convective heat transfer from smooth circular cylinders. Advances in Heat Transfer. Vol 11. p199-264

Pruppacher, H.R., and J.D. Klett, 1978: Microphysics of Clouds and Precipitation. D.Reidel Publishing Co. Boston. 714pp

Rogers, R.R., 1976: A Short Course in Cloud Physics. Pergamon Press. Oxford. 227pp

Schaefer, V.J., 1946: The production of ice crystals in a cloud of supercooled water droplets. Science. Vol 104. p457-459

Schaefer, V.J., 1949: The formation of ice crystals in the laboratory and the atmosphere. Chemical Reviews. Vol 44. p291-320

Schaefer, V.J., 1968: The early history of weather modification. Bulletin of the American Meteorological Society. Vol 49. p337-342

Schaefer, V.J., 1976: After Twenty-Nine Years - A Proposal. Journal of Weather Modification. Vol 8. p190-196

Silverman, B.A., 1979: The Design Of HIPLEX-1. A randomized rain augmentation experiment on summer cumulus congestus clouds on the Montana high plains. Bureau of Reclamation, Department of the Interior. Tech. Report, 271pp.

Sroka, M., 1972: Design of an Atmospheric Icing Tunnel. Unpublished MSc. Thesis, University of Alberta, Department of Mechanical Engineering. 74pp

Weast, R.C., ed., 1964: CRC Handbook of Chemistry and Physics, 45th edition. Chemical Rubber Company Press, Cleveland, Ohio.

Zukauskas, A., 1972: Heat Transfer from Tubes in Crossflow. Advances in Heat transfer, Vol 8. p93-160

## APPENDIX A

### Determination of the Nusselt Numbers from Experimental Observations

A method of obtaining a relationship between the Nusselt and Reynolds numbers directly from experimental observations was explored. Equation 10 applied to the dry conditions was re-arranged as:

$$Nu = \frac{dD}{dt} \frac{\rho_c L_\delta}{2k_a} \frac{D}{(t_s - t_a)} \qquad (1)$$

A series of four experiments conducted in dry air (8, 9, 14, and 19) was used to calculate the Nusselt number. A three point averaging filter was applied to the observations of dD/dt , to smooth out the large variations. The resultant smoothed values were then inserted in the above expression and a Nusselt number calculated. Corresponding Reynolds numbers computed from the experimental data, were substituted into the Zukauskas expression:

$$Nu = 0.26\ Re^{0.6} \qquad (2)$$

The results of the calculations are shown in Figure 27 in the form of a scatter diagram. The Nusselt number determined using the Zukauskas expression is plotted on the abscissa, while the Nusselt number obtained from experiments is plotted on the ordinate.

The 1:1 line is superimposed on the data. A linear regression analysis was performed on the data using the method of least squares. A correlation coefficient of 0.7 was calculated.

The Nusselt calculated from the experiments seems smaller than the Nusselt from the Zukauskas. This is consistent with the observation that the sublimation rate experimentally is generally lower than that predicted by the model. Errors in estimating the change in diameters explain why the scatter seems largest at the largest Nu. These results suggest that the observational data are not good enough to derive Nu.

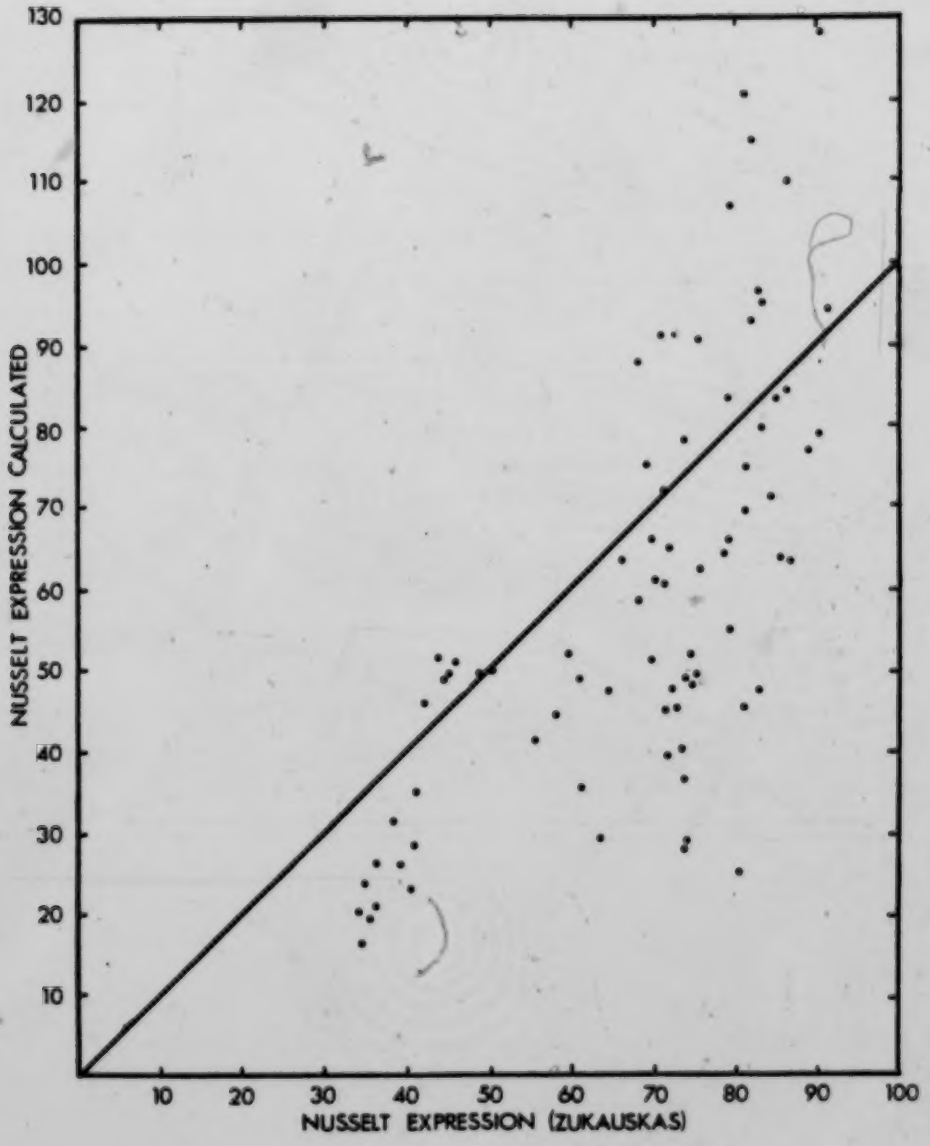


Figure 27

Scatter Diagram of Nusselt Calculations

## APPENDIX B

### Derivation of the $Q_{es}$ Term

The total latent heat transfer due to sublimation of water vapor onto the dry ice can be expressed as:

$$Q_{es} = h_m l_s \pi D L (\rho_a - \rho_s) \qquad (1)$$

where $h_m$ is the mass transfer coefficient, and $\rho_a$ and $\rho_s$ are the water vapor densities (absolute humidity) in the ambient environment and at the surface of the pellet.

The equation of state for dry air can be expressed as:

$$p_d = \rho R' T \qquad (2)$$

where $R'$ is the specific gas constant for dry air.

Water vapor in the atmosphere behaves as an ideal gas to a good approximation and its equation of state can be written as:

$$e = \rho_v R_v T \qquad (3)$$

where e is the partial pressure of the water vapor, $\rho_v$ is the vapor density and $R_v$ is the specific gas constant for water vapor.

The total air pressure P, according to Dalton's Law is equal to the sum of the partial pressures of the dry air and the water vapor.

$$P = p_d + e \qquad (4)$$

Then the equation of state for dry air can be re-written as:

$$\rho = \frac{(P-e)}{R'T} \qquad (5)$$

Considering the ratio of $\rho_v/\rho$:

$$\frac{\rho_v}{\rho} = \varepsilon\frac{e}{P-e} \approx \varepsilon\frac{e}{P} \qquad (6)$$

where $\varepsilon = \frac{R'}{R_v}$

or

$$\rho_v \approx \rho\ \varepsilon\frac{e}{P} \qquad (7)$$

The mass transfer coefficient $h_m$ in equation 1 can be given by:

$$Sh = \frac{h_m D}{\mathcal{D}_{wa}} \qquad (8)$$

where Sh is the Sherwood number, and $\mathcal{D}_{wa}$ is the diffusivity of water vapor in air.

Using the result that the vapor density can be related to vapor pressure according to equation 7, equation 1 can be re-written as:

$$Q_{es} = k_m l_s \pi DL(e_a - e_s) \qquad (9)$$

where $k_m = h_m \frac{\varepsilon\rho}{P}$

Substituting for $h_m$ according to equation 8, the mass transfer coefficient $k_m$ can be expressed as:

$$k_m = Sh\ \mathcal{D}_{wa}\ D^{-1}\ \frac{\varepsilon\rho}{p} \qquad (10)$$

or

$$k_m = \mathcal{D}_{wa}\ D^{-1}\ Sh\ \varepsilon R'^{-1} T^{-1} \qquad (11)$$

since $\varepsilon = \frac{R'}{R_v}$

then the mass transfer coefficient may be expressed as:

$$k_m = \mathcal{D}_{wa}\ D^{-1}\ Sh\ R_v^{-1}\ T^{-1} \qquad (12)$$

Now consider:

$$\frac{k_m}{h} = \frac{\mathcal{D}_{wa}\ D^{-1}\ Sh\ R_v^{-1}\ T^{-1}}{k_a\ D^{-1}\ Nu} \qquad (13)$$

$$\frac{k_m}{h} = \frac{\mathcal{D}_{wa}\ R_v^{-1}\ T^{-1}}{k_a} \left(\frac{Sh}{Nu}\right) \qquad (14)$$

since $Sh = cRe^m\ Sc^n$ ; and $Nu = cRe^m\ Pr^n$ , where Sc is the Schmidt number defined as $\nu/\mathcal{D}_{wa}$ ; and Pr is the Prandtl number defined as $\nu/\kappa$ . hence:

$$\frac{k_m}{h} = \frac{\mathcal{D}_{wa}\ R_v^{-1}\ T^{-1}}{k_a} \left(\frac{Sc}{Pr}\right)^n \qquad (15)$$

however $k_a = \kappa\rho\ c_p$ . Where $\kappa$ is the thermal diffusivity.

Then equation 15 can be re-written as:

$$\frac{k_m}{h} = \left(\frac{D_{wa}}{\kappa}\right) \frac{R_v^{-1}\ T^{-1}}{\rho\ c_p} \left(\frac{Sc}{Pr}\right)^n \qquad (16)$$

$$\frac{k_m}{h} = \left(\frac{D_{wa}}{\kappa}\right)\left(\frac{Sc}{Pr}\right)^n \frac{\varepsilon}{Pc_p} \qquad (17)$$

or

$$k_m = h\left(\frac{Pr}{Sc}\right)^{1-n} \frac{\varepsilon}{Pc_p} \qquad (18)$$

Hence, using a value of 0.37 for the exponent n (Morgan, 1975), equation 9 can finally be written as:

$$Q_{es} = \pi DLh\left(\frac{Pr}{Sc}\right)^{.63} \frac{\varepsilon I_s}{Pc_p} (e_a(t_a)-e_s(t_s)) \qquad (19)$$

## APPENDIX C

## An Order of Magnitude Analysis of the Heat Balance Equation

A numerical example is presented and the relative magnitudes of the $Q_c$, $Q_{es}$, $Q_r$ and $Q_d$ terms are evaluated. The following conditions have been used in the calculations:

$D = 1.5\times10^{-2}$ m $\quad L = 5.0\times10^{-2}$ m $\quad V = 14$ ms$^{-1}$

$t_a = 20^0$C $\quad t_s = -100^0$C $\quad \rho_a = 1.275$ kgm$^{-3}$

$\sigma = 5.67\times10^{-8}$ Wm$^{-2}$ K$^{-4}$ $\quad \pi = 3.14159$

$h = k_a Nu D^{-1}$ Wm$^{-2}$ K$^{-1}$

$k_a = 2.43\times10^{-2} + 7.3\times10^{-4}(t_a)$ Wm$^{-1}$ K$^{-1}$

$Nu = 0.26Re^{0.6}$

$Re = VD\nu^{-1}$

$\nu = \mu_a \rho_a^{-1}$ m$^2$s$^{-1}$

$\mu_a = 1.718\times10^{-5} + 5.1\times10^{-7}(t_a)$ kgm$^{-1}$ s$^{-1}$

$\mu_a = 2.738\times10^{-5}$ kgm$^{-1}$ s$^{-1}$

$\nu = 2.147\times10^{-5}$ m$^2$s$^{-1}$

$Re = 9.779\times10^3$

$Nu = 64.4$

$k_a = 3.89\times10^{-2}$ Wm$^{-1}$ K$^{-1}$

$h = 1.67\times10^2$ Wm$^{-2}$K$^{-1}$

The heat transfer due to conduction and convection is evaluated as:

$$Q_c = \pi DLh(t_s - t_a)$$

$$Q_c = -47.2 \text{ Watts}$$

The heat transfer due to sublimation of water vapor onto the dry ice, is evaluated as:

$$Q_{es} = -\pi DLh\left(\frac{Pr}{Sc}\right)^{.63} \frac{\varepsilon l_s}{Pc_p} (e_a(t_a)-e_s(t_s))$$

where $\varepsilon$ = 0.622

$Pr$ = 0.711

$Sc$ = 0.595

$c_p$ = $1.005 \times 10^3$ $Jkg^{-1} K^{-1}$

$l_s$ = $2.823 \times 10^6$ $Jkg^{-1}$

$P$ = 930 mb

$e_a(t_a)$ = 23.373 mb

$$Q_{es} = -19.3 \text{ Watts}$$

The heat transfer due to radiation is evaluated as:

$$Q_r = -\sigma(T_a^4 \varepsilon_a - T_s^4 \varepsilon_s) \pi DL$$

where the emissivities are assumed to be 1

$T_a$ = 293.15 K

$T_s$ = 173.15 K

$$Q_r = -0.867 \text{ Watts}$$

The heat transfer due to the droplets is evaluated as:

$$Q_d = -(c_w R_w(t_a - 0^\circ C) + R_w L_f + c_i R_w(0^\circ C - t_s))$$

where $c_w$ = $4.19 \times 10^3$ $Jkg^{-1} K^{-1}$

$c_i$ = $1.74 \times 10^3$ $Jkg^{-1} K^{-1}$

$L_f$ = $3.34 \times 10^5$ $Jkg^{-1}$

$R_w$ is the mass flux of droplets collected per unit time, and is defined as: EWwDL

Where E is the collection efficiency, assumed to be 1 (this is an over-estimate. A precise value cannot be obtained because the droplet size spectrum was not measured.), V is the velocity, and w is the liquid water content. A value typical for a small cumulus cloud is of the order $1.0 \times 10^{-3}$ $kgm^{-3}$.

Therefore $R_w = 1.05 \times 10^{-5}$ $kgs^{-1}$.

In the term each component is evaluated as

a = 0.88 Watts

b = 3.51 Watts

c = 1.83 Watts

$$Q_d = -6.22 \text{ Watts}$$

It can be seen that radiation only contributes at the most a small percentage to the total heat exchange and may be ignored. The heat due to the droplets is not a small amount as can be seen by the calculations. The contribution to the heat balance, though, is unknown since we do not know at what stage in the cooling process the droplets leave the surface. In addition, during the experiments ice accretion was not observed on the surface of the pellet. It is for these reasons that the heat contribution due to the droplets is ignored.

## APPENDIX D

## Analytic Solution to

## Sublimation Rate Expression

The sublimation rate expression (equation 10), is written as:

$$\frac{dD}{dt} = \frac{2k_a Nu}{\rho_c L_\delta D}\left[(t_s - t_a) - \left(\frac{Pr}{Sc}\right)^{.63} \frac{\varepsilon l_s}{Pc_p} e_a(t_a)\right] \qquad (1)$$

the terms within the square brackets are a constant with time, say -C. Then:

$$\frac{dD}{dt} = - \frac{2k_a Nu}{\rho_c L_\delta D} C \qquad (2)$$

Substituting for the Reynolds and Nusselt numbers,

$$Re = \frac{VD}{\nu} \qquad Nu = 0.26\ Re^{0.6} \qquad (3)$$

Then:

$$\frac{dD}{dt} = - \frac{2k_a V^{0.6}\ D^{0.6}\ 0.26}{\rho_c L_\delta D \nu^{0.6}} C$$

$$\frac{dD}{dt} = - KD^{-0.4} \qquad (4)$$

where:

$$K = \frac{2k_a V^{0.6}\ 0.26}{\rho_c L_\delta \nu^{0.6}} C \qquad (5)$$

which is also a constant in the wind tunnel, but not in the free fall experiments.

This expression may be integrated to give:

$$D = (D_i^{1.4} - 1.4Kt)^{1/1.4} \qquad (6)$$

where $D_i$ is the initial diameter.

APPENDIX E

Derivation of the Terminal Velocity

for a Cylindrical Object

The forces acting on a cylindrical object falling freely in air are depicted in the following schematic.

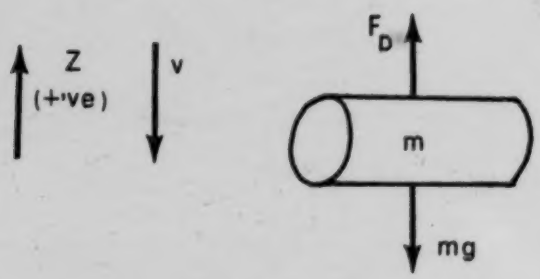


The equation of motion for this cylindrical object, neglecting buoyancy which is expected to be small for dry ice pellets, can be written as:

$$- ma = - \frac{mdV}{dt} = mg - F_D \qquad (1)$$

where m is the mass of the cylinder, g is the acceleration of gravity, and $F_D$ is the drag force. The negative sign appears on the left hand side of this expression because V is considered to be negative when directed downwards.

The drag force (Huschke,1959) can be written as:

$$F_D = 1/2\ A_x C_D \rho_a V^2 \qquad (2)$$

where $A_x$ is the cross-sectional area of the body normal to the airstream. For a cylinder this is:

$$A_x = D\ L \qquad (3)$$

where D is the diameter of the cylinder, and L is the length.

Hence,the drag force acting on a freely falling cylinder, oriented with its axis horizontal, can be written as:

$$F_D = 1/2\ DLC_D \rho_a V^2 \qquad (4)$$

The mass of the cylinder is:

$$m = \frac{\pi D^2 L \rho_c}{4} \qquad (5)$$

Substituting the expressions for the drag force and the mass of the cylinder, into the equation of motion, we obtain:

$$g - kV^2 = -\frac{dV}{dt} \qquad (6)$$

where

$$k = \frac{2C_D\rho_a}{\pi D\rho_c} \qquad (7)$$

The terminal velocity $V=V_T$ occurs when the net force acting on the cylinder is zero.

hence

$$-a = -\frac{dV}{dt} = 0 = g - kV_T^2 \qquad (8)$$

or

$$V_T^2 = \frac{g}{K} \qquad (9)$$

The terminal velocity for a freely falling cylinder can therefore be expressed as:

$$V_T = \left(\frac{\pi\rho_c gD}{2C_D\rho_a}\right)^{1/2} \qquad (10)$$

# APPENDIX F

## Computer Program Listings

This appendix contains the FORTRAN listings for the computer routines used in and developed for this thesis.

```
      C
      C       SUBLIME.FOR
      C
      C*************************************************************************
      C
      C     THE NUMERICAL SIMULATION OF DRY ICE SUBLIMATION USING
      C     HEAT TRANSFER RELATIONSHIPS.
      C
      C     THIS MODEL IS VALID FOR CYLINDRICAL PARTICLES.
      C
      C
      C*************************************************************************
      C
      C
      C
            REAL NMASS,NRAD,NUSELT,MBCON,INCON,MU,NU,MASS
            REAL NDIAM,LHS,KA,NUMR,KAPPA,LHW
      C
      C     DEFINE SOME CONSTANTS
      C
            RHOCO2=1.40
            CM=2.54
            MBCON=1000.
            INCON=2.49082E03
            LHS=587E07
            LHW=0.0
            PI=3.14159
            RE=0.
            NUSELT=0.
      C
      C
      C
      C*************************************************************************
      C
      C          FORMAT STATEMENTS
      C
      C*************************************************************************
      C
      C
      C
      1     FORMAT(1X,'INPUT---TIME INT.,CYL.DIA,CYL.LEN.')
      2     FORMAT(1X,'INTRODUCE INITIAL CONDITIONS---TA,PA,DELP,TS,VEL,WET')
      12    FORMAT('1',42X,'THE NUMERICAL SIMULATION OF DRY ICE SUBLIMATION',/
           +/)
      16    FORMAT(' ',33X,'DRY CASE---SPRAYS OFF',//)
      17    FORMAT(' ',33X,'WET CASE---SPRAYS ON',//)
      18    FORMAT(' ',33X,'TIME INTERVAL (DELT)=',F4.2,' SECONDS',//)
      13    FORMAT(' ',9X,'INITIAL CONDITIONS:',4X,'PELLET TEMPERATURE:',9X,
           +F6.1,1X,'CELSIUS',/,33X,'DRY ICE DENSITY:',14X,
           +F5.2,1X,'GM/CM**3',/,33X,'CYLINDRICAL RADIUS:',11X,F5.2,1X,'CM',/,
           +33X,'CYLINDRICAL LENGTH:',11X,F5.2,1X,'CM',/,33X,'CYLINDRICAL DIAM
           +ETER:',9X,F5.2,1X,'CM',/,33X,'AMBIENT TEMPERATURE:',10X,F6.
           +2,1X,'CELSIUS',/,33X,'AMBIENT PRESSURE:',13X,F5.1,1X,'MB',/,33X,
           +'WIND TUNNEL VELOCITY:',9X,F5.2,1X,'M/SEC')
      15    FORMAT('1',15X,'TIME',15X,
           +'DIAMETER',15X,'MASS',15X,'REYNOLDS',15X,'NUSSELT',/,
           +14X,'(SEC)',17X,'(CM)',17X,'(GM)',/)
      14    FORMAT(13X,F7.2,15X,F8.6,14X,F6.2,14X,F8.2,14X,F8.2)
      666   FORMAT(2F10.4)
```

```
      888   FORMAT(1X,4F20.6)
C
C
C
C     INPUT CYLINDRICAL LENGTH AND RADIUS (CM) AND TIME INTERVAL (SEC) .
C
C
      10    WRITE(6,1)
            CALL FREAD(5,'3R:',DELT,CYLD,CYLL)
            IF (DELT.EQ.0.) GO TO 90
            TIME=0.0
            J=0
            LINE=0
C
C
C-----  CALCULATE CYLINDRICAL MASS .(CMAS.)
C
C
            CRM=CYLD/2.
            NDIAM=CYLD
            CMAS=PI*((NDIAM*NDIAM)/4)*CYLL*RHOCO2
C
C
C     INTRODUCE INITIAL CONDITIONS: TA- AMBIENT TEMP. IN CELSIUS.
C                                    PA- AMBIENT PRESSURE IN MB.
C                                  DELP- DYNAMIC PRESSURE INCHES
C                                    TS- PELLET TEMPERATURE IN CELSIUS
C                                    VEL- VELOCITY IN M/S  DETERMINED
C                                    WET- WET/DRY CASE?
C
C
            WRITE(6,2)
            CALL FREAD(5,'6R:',TA,PA,DELP,TS,VEL,WET)
C
            TBAR=(TA+TS)/2.
            TBK=TBAR+273.16
            TAK=TA+273.16
            TSK=TS+273.16
            PAT=PA*(0.9862E-03)
C
            RD=0.287E07
            P=PA*MBCON
            RHOA=P/(RD*TAK)
C
            IF(DELP.EQ.0.) GO TO 100
            V=(2*DELP*(INCON/RHOA))**(1./2.)
            VM=V/100.
            GO TO 11
      100   V=VEL*100.
            VM=VEL
C
      11    WRITE(7,12)
            IF(WET.EQ.0.) WRITE(7,16)
            IF(WET.EQ.1.) WRITE(7,17)
            WRITE(7,18) DELT
C
            WRITE(7,13) TS,RHOCO2,CRM,CYLL,NDIAM,TA,PA,VM
            WRITE(7,15)
            LINE=LINE+3
C
```

```
121           WRITE(7,14) TIME,NDIAM,CMAS,RE,NUSELT
122           LINE=LINE+1
123     C
124           TIME=TIME+DELT
125           J=TIME
126     C
127     C
128     C----- COMPUTE THE THERMAL CONDUCTIVITY OF AIR.
129     C
130     C
131           KA=2.43E-02+(7.3E-04*TA)
132           KA=KA*1.0E05
133     C
134           CP=1.005E07
135     C----- CALCULATE KINEMATIC VISCOSITY.
136     C
137     C
138           MU=1.718E-05+(5.1E-07*TA)
139           MU=MU*10.
140     C
141           NU=MU/RHOA
142     C
143     C
144           PR=0.711
145           SC=.595
146     C
147     C
148     C     SEPARATE HEAT TRANSFER TERMS  CALCULATED
149     C
150     C
151           QC=(TS-TA)/LHS
152     C
153     C
154     C
155     C
156           IF(WET.EQ.0.) GO TO 50
157     C
158     C
159     C     A  POLYNOMIAL EXPRESSION (LOWE,1976) USED
160     C      TO COMPUTE SAT. VAP. PRESS.
161     C
162           A0=6.107799961
163           A1=4.436518521E-01
164           A2=1.428945805E-02
165           A3=2.650648471E-04
166           A4=3.031240396E-06
167     C
168           T=TA
169           EATA=A0+T*(A1+T*(A2+T*(A3+A4*T)))
170     C
171           S0=676.967
172           S1=-0.0680427
173           S2=-0.120855E-02
174           S3=-0.518213E-05
175           S4=-0.249304E-07
176     C
177           TM=TS
178           LHW=S0+TM*(S1+TM*(S2+TM*(S3+S4*TM)))
179           WRITE(6,666) EATA,LHW
180     C
```

```
181           LHW=(LHW/0.2389)*1.0E07
182           EPS=0.622
183           QE1=(PR/SC)**(0.63)
184           QE2=-(EPS)/(PA*CP)*(LHW/LHS)
185           QE3=EATA
186           QE=QE1*QE2*QE3
187           GO TO 20
188     50    QE=0.0
189     C
190     C----- CALCULATE REYNOLDS NUMBER FOR NEW DIAMETER.
191     C
192     C
193     20    RE=V*NDIAM/NU
194     C
195     C
196     C
197     C----- USING THE SUBLIMATION EXPRESSION DERIVED COMPUTE CHANGE
198     C        IN MASS,HENCE CHANGE IN DIAMETER, AFTER TIME DELTA.
199     C
200     C
201     C
202     C
203     C      NUSSELT RELATION ACCORDING TO ZUKAUSKAS
204     C     APPROPRIATE FOR REYNOLDS RANGE 10**3-10**5
205     C
206           NUSELT=0.23*(RE**0.6)
207     C
208           CONST=(2*KA*NUSELT)/RHOCO2
209           DELD=((CONST/NDIAM)*(QC+QE))*DELT
210           NDIAM=NDIAM+DELD
211           NMASS=PI*RHOCO2*CYLL*((NDIAM*NDIAM)/4)
212     C
213           IF(NDIAM.LE.0.) GO TO 25
214           GO TO 30
215     25    NDIAM=0.0
216           NMASS=0.0
217     C
218     C
219     30    IF((TIME-J).EQ.0) GO TO 200
220           GO TO 21
221     200   WRITE(7,14) TIME,NDIAM,NMASS,RE,NUSELT
222     C
223           WRITE(8,888) TIME,DELD,QC,QE
224     C
225           LINE=LINE+1
226           IF(LINE.EQ.56) GO TO 31
227     21    IF(NDIAM.EQ.0.) GO TO 10
228           TIME=TIME+DELT
229           J=TIME
230           GO TO 20
231     31    LINE=0
232           WRITE(7,15)
233           WRITE(7,14) TIME,NDIAM,NMASS,RE,NUSELT
234           LINE=LINE+4
235           TIME=TIME+DELT
236           J=TIME
237           GO TO 20
238     C
239     90    STOP
240           END
```

```
      C
      C       CYLDRP.FOR
      C
      C*************************************************************************
      C
      C     THE NUMERICAL SIMULATION OF DRY ICE SUBLIMATION USING
      C     HEAT TRANSFER RELATIONSHIPS.
      C
      C     THIS MODEL IS VALID FOR CYLINDRICAL PARTICLES.
      C     FALLING THROUGH AN ATMOSPHERE.
      C
      C
      C
      C*************************************************************************
      C
      C
      C
            REAL NMASS,NRAD,NUSELT,MBCON,INCON,MU,NU,MASS
            REAL NDIAM,LHS,KA,NUMR,KAPPA,H,LAPSE,KELVIN
      C
      C     DEFINE SOME CONSTANTS
      C
            RHOCO2=1.40
            CP=1.005E07
            TS=-78.0
            CM=2.54
            MBCON=1000.
            PI=3.14159
            LAPSE=1./152.
            RD=0.278E07
            GRAV=980.616
            CLAPSE=LAPSE/100.
            DENM=CLAPSE*RD
            EXP=GRAV/DENM
            LHS=587E07
            KELVIN=273.16
      C
      C
      C
      C*************************************************************************
      C
      C          FORMAT STATEMENTS
      C
      C*************************************************************************
      C
      C
      C
      1     FORMAT(1X,'INPUT---TIME INT.,CYL.DIA,CYL.LEN.,DRAG')
      2     FORMAT(1X,'INTRODUCE INITIAL CONDITIONS---TA,PA,H,WET')
      12    FORMAT('1',42X,'THE NUMERICAL SIMULATION OF DRY ICE SUBLIMATION'./
           +/)
      777   FORMAT(' ',33X,'DRAG COEFFICIENT:',F5.2,/)
      13    FORMAT(' ',9X,'INITIAL CONDITIONS:',/,33X,'DRY ICE DENSITY:',14X,
           +F5.2,1X,'GM/CM**3',/,33X,'CYLINDRICAL RADIUS:',11X,F5.2,1X,'CM',/,
           +33X,'CYLINDRICAL LENGTH:',11X,F5.2,1X,'CM',/,33X,'CYLINDRICAL DIAM
           +ETER:',9X,F5.2,1X,'CM',/,33X,'AMBIENT TEMPERATURE:',10X,F6.
           +2,1X,'CELSIUS',/,33X,'AMBIENT PRESSURE:',13X,F5.1,1X,'MB',/,33X,
           +'INITIAL DROP HEIGHT:',10X,F8.1,1X,'(FT MSL)',///,40X,'TIME',
           +5X,'TEMP',5X,'PRESSURE',5X,'HEIGHT',5X,'DIAMETER',/,40X,'(SEC)'
```

```
60          +,5X,'(C)',7X,'(MB)',6X,'(FT MSL)',5X,'(CM)')
61     14   FORMAT(38X,F7.3,4X,F5.1,6X,F5.1,5X,F8.1,6X,F8.6)
62     C
63     C
64     C    INPUT CYLINDRICAL LENGTH AND RADIUS (CM) AND TIME INTERVAL (SEC) .
65     C
66     C
67     10   WRITE(6,1)
68          CALL FREAD(5,'4R:',DELT,CYLD,CYLL,DRAG)
69     C
70          IF (DELT.EQ.0.) GO TO 90
71          TIME=0.0
72     C
73     C
74     C
75     C
76          CRM=CYLD/2.
77          NDIAM=CYLD
78          CLM=CYLL
79          CMAS=PI*((NDIAM*NDIAM)/4)*CYLL*RHOCO2
80     C
81     C
82     C    INTRODUCE INITIAL CONDITIONS: TA- AMBIENT TEMP. IN CELSIUS.
83     C                                  PA- AMBIENT PRESSURE IN MB.
84     C                                   H- DROP HEIGHT (FT. MSL)
85     C
86     C
87          WRITE(6,2)
88          CALL FREAD(5,'4R:',TA,PA,H,WET)
89     C
90          TAK=TA+KELVIN
91          PAT=PA*(0.9862E-03)
92     C
93          P=PA*MBCON
94          RHOA=P/(RD*TAK)
95          WRITE(7,12)
96          WRITE(7,777) DRAG
97     C
98          WRITE(7,13) RHOCO2,CRM,CLM,NDIAM,TA,PA,H
99          WRITE(7,14) TIME,TA,PA,H,NDIAM
100    C
101    C
102    C
103    C    COMPUTATION OF TERMINAL VELOCITY,MEAN TEMP.,MEAN PRESSURE,
104    C       AND DISTANCE FALLEN DURING THE TIME INTERVAL SPECIFIED.
105    C
106    C
107    20   X=PI*RHOCO2*GRAV*CRM
108         Y=DRAG*RHOA
109         TV=SQRT(X/Y)
110         DIST=TV*DELT
111         H=H-(DIST*0.03281)
112         DISTM=DIST/100.
113         TNEW=TA+(LAPSE*DISTM)
114         TNAB=TNEW+KELVIN
115         PNEW=PA*((TNAB/TAK))**EXP
116         PMEAN=(PA+PNEW)/2.
117         TMEAN=(TA+TNEW)/2.
118          TAK=TNAB
119         TMK=TMEAN+KELVIN
```

```
120             TA=TNEW
121             PA=PNEW
122            P=PA*MBCON
123            PAT=PA*(0.9862E-03)
124            TIME=TIME+DELT
125            RHOA=P/(RD*TAK)
126            PM=PMEAN*MBCON
127            RHOAM=PM/(RD*TMK)
128       C
129       C
130       C
131       C----- COMPUTE THE THERMAL CONDUCTIVITY OF AIR.
132       C
133       C
134            KA=2.43E-02+(7.3E-04*TMEAN)
135            KA=KA*1.0E05
136       C
137       C----- CALCULATE KINEMATIC VISCOSITY.
138       C
139       C
140            MU=1.718E-05+(5.1E-07*TMEAN)
141            MU=MU*10.
142       C
143            NU=MU/RHOAM
144       C
145       C
146            PR=0.711
147            SC=0.595
148       C
149       C
150       C     SEPARATE HEAT TRANSFER TERMS  CALCULATED
151       C
152       C
153            QC=(TS-TMEAN)/LHS
154       C
155       C
156       C
157       C
158            IF(WET.EQ.0.) GO TO 50
159       C
160       C
161       C     A  POLYNOMIAL EXPRESSION (LOWE,1976) USED
162       C      TO COMPUTE SAT. VAP. PRESS.
163       C
164            A0=6.107799961
165            A1=4.436518521E-01
166            A2=1.428945805E-02
167            A3=2.650648471E-04
168            A4=3.031240396E-06
169       C
170            T=TMEAN
171            EATA=A0+T*(A1+T*(A2+T*(A3+A4*T)))
172       C
173            S0=676.967
174            S1=-0.0680427
175            S2=-0.120855E-02
176            S3=-0.518213E-05
177            S4=-0.249304E-07
178       C
179            TM=TS
```

```
      LHW=SO+TM*(S1+TM*(S2+TM*(S3+S4*TM)))
C
      LHW=(LHW/0.2389)*1.0E07
      EPS=0.622
      QE1=(PR/SC)**(0.63)
      QE2=-(EPS)/(PMEAN*CP)*(LHW/LHS)
      QE3=EATA
      QE=QE1*QE2*QE3
C
      GO TO 21
50    QE=0.0
C
C----- CALCULATE REYNOLDS NUMBER FOR NEW DIAMETER.
C
C
21    RE=TV*NDIAM/NU
C
C
C
C----- USING THE SUBLIMATION EXPRESSION DERIVED COMPUTE CHANGE
C       IN MASS,HENCE CHANGE IN DIAMETER, AFTER TIME DELTA.
C
C
C
C
C     NUSSELT RELATION ACCORDING TO ZUKAUSKAS
C    APPROPRIATE FOR REYNOLDS RANGE 10**3-10**5
C
      NUSELT=0.23*(RE**0.6)
C
      CONST=(2*KA*NUSELT)/RHOCO2
      DELD=((CONST/NDIAM)*(QC+QE))*DELT
      NDIAM=NDIAM+DELD
      NMASS=PI*RHOCO2*CYLL*((NDIAM*NDIAM)/4)
C
      IF(NDIAM.LE.0.) GO TO 25
      GO TO 30
25    NDIAM=0.0
C
C
30    WRITE(7,14) TIME,TA,PA,H,NDIAM
      IF(NDIAM.EQ.0.) GO TO 10
      IF(H.LE.3000.) GO TO 10
      GO TO 20
C
C
90    STOP
      END
```